


Document NWPSAF-MO-VS-052

Version 1.0

18/11/15

Investigation into the partitioning of cloud signals into IASI reconstructed radiances

Olaf Stiller, Fiona Smith, and Christina Köpken-Watts

The EUMETSAT Network of Satellite Application Facilities	 NWP SAF Numerical Weather Prediction	Investigation into the partitioning of cloud signals into IASI reconstructed radiances	Doc ID : NWPSAF-MO-VS-52 Version : 1.0 Date : 18/11/15
---	--	--	--

Investigation into the partitioning of cloud signals into IASI reconstructed radiances

Olaf Stiller¹, Fiona Smith²,
Christina Köpken-Watts¹

¹Deutscher Wetterdienst; ²Met Office

This documentation was developed within the context of the EUMETSAT Satellite Application Facility on Numerical Weather Prediction (NWP SAF), under the Cooperation Agreement dated 29 June 2011, between EUMETSAT and the Met Office, UK, by one or more partners within the NWP SAF. The partners in the NWP SAF are the Met Office, ECMWF, KNMI and Météo France.

Copyright 2015, EUMETSAT, All Rights Reserved.

Change record			
Version	Date	Author / changed by	Remarks
1.0	18/11/15	Olaf Stiller, Fiona Smith, and Christina Köpken-Watts	Final report.

EUMETSAT NWP SAF visiting scientist report:

Olaf Stiller*, Fiona Smith⁺, Christina Köpken-Watts*

*Deutscher Wetterdienst, Offenbach, Germany

⁺Met Office, Exeter, United Kingdom

November 16, 2015

Foreword

This report describes the outcome of a 2 weeks stay of Olaf Stiller as a visiting scientist within the NWP SAF program at the Met Office in August/September 2015. It compares statistical properties of IASI radiances which were reconstructed from principal component scores with those of the original measurements for the respective channels. The emphasis is on how these statistical properties change with different regimes of cloudiness and more particular, if one can find any evidence that, for reconstructed radiances, cloud information from low level clouds could be aliased into channels for which the raw radiances have their sensitivity functions *above* the cloudy region (i.e., the raw radiances are not affected by the cloud).

Due to the short time frame, it was decided to focus only on bands 1 and 2 which, in an NWP context, are the by far most studied and used data. For these data, a large number of figures have been produced during this study many of which are shown in this report. Again, due to the shortness of the available time, not all details of the computed (and presented) data could be fully understood and/or discussed. Below, for the sake of completeness, some plots have been included which actually receive very little discussion. (Most of the discussions are actually restricted to band 1.) To make optimal use of the available time, it was deemed most valuable to focus the discussions on only a few aspects which looked interesting and which are hoped to give some useful information for future statistical studies of hyperspectral sounder data in the context of principal components analysis. Particular attention was given to aspects which were found to make the interpretation for some of the statistical data computed for this study difficult.

1 Introduction

During the last years, an increasing body of work has demonstrated the value of principal component (PC) analysis of satellite data from hyperspectral sounders with respect to data dissemination (data compression) and applications in numerical weather prediction (NWP) (see, e.g., *Hilton et al. (2009)*; *Atkinson et al. (2010)*; *Hilton et al. (2012)*; *Guedj et al. (2015)*). A recent trend appears to favor NWP applications involving reconstructed radiances (RRs) rather than making direct use of the PC scores themselves.

Of course, like any approximation method, PC decomposition also has limitations whose identification is, however, often not straight forward and requires thorough investigation as the performance of these data may be different in different circumstances (different data regimes). Therefore, while the work carried out so far has demonstrated the usefulness of these data, further testing for increasing our understanding of their behavior in different types of situations should continue.

The work presented here was motivated by the question whether for channels which themselves are not directly influenced by clouds (i.e., their sensitivity functions have non-negligible values only in cloud free regions) the reconstructed radiances could still be influenced by clouds which are beneath their sensitivity regions. This type of aliasing of lower level cloud information into higher peaking channels could, in principle, occur since reconstructed radiance are a linear combination of a large number of the other channels. So, when using information from cloud affected channels to reconstruct channels which are not influenced by clouds, it is not unreasonable to ask whether this could in some situations have a negative effect on the reconstructed observations.

1.1 Principal Components decomposition

1.1.1 The ideas

Reconstructed radiances are obtained through a principal component (PC) decomposition which on one hand can be simply regarded as a means of data compression. Considering a large data set which contains a large number of n dimensional arrays \mathbf{y} (where n is a large number), an analysis of the $n \times n$ dimensional covariance matrix \mathbf{C} often reveals that the number of directions in which the data set exhibits significant variance is much smaller than n . Data compression is then achieved by using only degrees of freedom with *substantial* variance for describing the elements of the data set (i.e., the arrays). These degrees of freedom, i.e., the (statistically independent) directions with the largest variance are the eigenvectors \mathbf{v}_i of \mathbf{C} which correspond to the largest eigenvalues λ_i . One hope is that by taking only the directions corresponding to the p largest eigenvalues (with $p \ll n$) each array of the data set can be described with *sufficient precision* and contains most of the information given by the data.

In the ideal case, when applying the formalism to noisy data arrays like observational IASI spectra, contributions from the other eigenvectors (i.e., those with smaller eigenvalues) which are truncated in the PC expansion contain only noise while all the useful signal is contained in the leading principal components. If this is the case the benefit of PC decomposition may go well beyond mere data compression.

Assessing whether those aims (sufficiently precise reproduction of observational information and/or suppression of noise) are actually achieved for a selected choice of PCs is, however, not a purely mathematical exercise but requires an in-depth knowledge about the nature of both the respective signal and the noise. In meteorology, comparing the data with their model counterparts (computed with the observation operators) plays a crucial role in this context. Particularly the fact, that observation operators for different IASI channels strongly overlap (and therefore the data should be correlated) gives some confidence that a strong data reduction (without losing much of the signal) should be possible. So far extensive studies and NWP applications have confirmed the great value of PC decomposition for these data. The short study presented here checked whether any weaknesses of the method could be identified for situations involving the coexistence of different regimes in a spectrum (i.e., the coexistence of channels affected and not affected by the presence of low level clouds).

1.1.2 Reconstructed Radiances

PC decomposition expresses the array of observations (radiance spectra) as a sum over the eigenvectors of the covariance matrix and then neglects all contributions but those from the dominant eigenvectors. Then, the projections of an array \mathbf{y} onto the selected eigenvectors, which are called the PC scores, in principle, characterize the full radiance spectrum \mathbf{y} within the approximation of the PC decomposition. For exploiting the wealth of information contained in the PC scores, observation operators (radiative transfer models) have been developed which directly compute the PCs from the state model vector of the NWP model. In principle, however, one is not restricted to directly using the PC scores but any (bijective!) linear combination of these scores contains the same information.

One pragmatic choice of linear combinations of the PC scores which are often used are reconstructed radiances (RR). I.e., for some selected channels, PC scores are computed back into radiance space where (if the PC decomposition works) the resulting RRs should resemble the original measurements (or raw radiances, also referred to in this report as “Raw”). While the RRs generally contain less information than the corresponding PC scores (the transformation between PC scores and raw radiances is in general not bijective), RRs have the great advantage that large parts of their processing can be performed similarly to the Raw data. In particular, cloud screening methods can be applied in a similar fashion.

While RRs strongly resemble raw radiances, their information content is theoretically much larger than for the corresponding set of raw radiances. Within the approximation of the PC decomposition and the rank and condition number of the transformation matrix, RRs contain information about the whole observational spectrum. Exploiting the full information content in a data assimilation context is, however, quite expensive as the corresponding observation operator would be relatively complex. Therefore, in practice, the forward operator for the raw radiances is usually also employed for the RRs.

1.1.3 Some features and limitations

PC decomposition represents the observational spectrum. i.e., the (n dimensional) vector \mathbf{y} by considering only the p vector space directions where the observational data set has the largest variance. More precisely, the full observational spectrum \mathbf{y} is approximated by a vector \mathbf{y}_{pc} which (for a given number of degrees of freedom p) minimizes the expectation value

$$\langle (\mathbf{y}_{pc} - \mathbf{y}) * (\mathbf{y}_{pc} - \mathbf{y}) \rangle \quad (1)$$

where “*” is the scalar product of the vectors, the brackets $\langle \dots \rangle$ denote the expectation value and \mathbf{y}_{pc} is the approximation of the observation vector resulting from the PC analysis (this is the full observation vector, below the term reconstructed radiances will be mostly denoted to a channel subset of \mathbf{y}_{pc} which is selected for usage within an assimilation system). For IASI radiances, the observations are first “normalized” by the multiplication square root $\mathbf{N}^{-\frac{1}{2}}$ of the instrument noise matrix \mathbf{N} (i.e., $\mathbf{y} \rightarrow \mathbf{N}^{-\frac{1}{2}}\mathbf{y}$) which is equivalent to introducing the scalar product $\mathbf{y} * \mathbf{v} \equiv \mathbf{y}^T \mathbf{N}^{-1} \mathbf{v}$.

Since Eq.(1) involves the global scalar product (i.e., of the full radiances) the method is particularly suited to cover all extended or collective \mathbf{y} structures (i.e., structures in observation space which involve a larger number of channels) and which are frequent while the description of localized features (involving only a very small number of channels) or very rare events is less obvious. Of

course, the great majority of very localized features must be caused by noise since IASI channels strongly overlap and many channels measure largely the same physical variables. The signal related to these channels should therefore generally lead to extended, i.e., collective \mathbf{y} structures and the great majority of very localized features should, indeed, be related to noise.

It is, however, a priori not completely obvious whether in certain situations, features which are small scale (i.e., features $\tilde{\mathbf{y}}$ for which the expectation value of the scalar product $\tilde{\mathbf{y}}^T \mathbf{N}^{-1} \tilde{\mathbf{y}}$ is small) could be of meteorological importance. While, in principle, such features might be well approximated by (linear combinations of) the chosen set of PCs, there is no guarantee that this is the case. In this context, e.g., transition regions between cloud affected and cloud free data require particular attention as they could exhibit such local properties whose representation by the PC decomposition might be problematic.

It should further be noted that PC analysis is probably most suited for representing data sets which correspond to multi-Gaussian fields. For more complex (“non-linear”) data sets the method is less efficient. For data sets which contain different regimes, the covariance matrix is generally given by a weighted average of the respective matrices corresponding to the respective regimes. Nevertheless, PC analysis selects the directions in observation space which have the largest contributions to the variance

$$\langle \mathbf{y}^T \mathbf{N}^{-1} \mathbf{y} \rangle \quad (2)$$

also for such mixed data sets. The description of the data may, however, require more PCs when the eigenvectors corresponding to different regimes differ. Generally, the sufficient representation of the different regimes requires different numbers of PCs, respectively and PCs which are needed for the signal in one regime may correspond to noise in the other. Still, if collective features are mostly related to the signal and localized features to noise, PC analysis should, in principle, also be able to adequately reproduce the signal for such data provided the employed number of PC scores is large enough.

1.2 1D Var retrievals (i.e., assimilations) of Cloud Variables

Below, statistics are grouped according to cloud parameters retrieved by the Met Office 1D Var system (see Pavelin et al. (2008)). Note that the Met office assimilation of IASI spectra is performed using brightness temperatures rather than radiances. The terms Raw and Reconstructed Radiances are therefore used descriptively and all values reported are in units of Kelvin. The forward model used in the 1D-Var analysis is the Radiative Transfer for TIROS Operational Vertical Sounder radiative transfer model (RTTOV, see Saunders et al. (2005); Matricardi et al. (2004)). As described in Pavelin et al. (2008), infrared cloud effects are obtained by running RTTOV in a somewhat simplistic mode where clouds are represented as grey bodies of negligible depth which can be fully described through two parameters, cloud fraction, CFr and cloud top pressure, CTP . These two parameters are added to the 1D Var atmospheric state vector and the retrieved values are passed to 4D Var where they are used as a fixed constraint on the radiative transfer calculation during assimilation.

It has to be stressed that the 1D Var system (whose results are used in this study) is currently used only as a preprocessing system for the 4D Var assimilation in the Met Office system. The preprocessing step passes on cloud variables and filters out all observations which are *significantly* influenced by the presence of clouds. More precisely, all channels that have more than 10% of their

Jacobians below the retrieved cloud top are excluded from the 4D Var assimilation step as the simplistic cloud model is not trusted to be sufficiently accurate. Accordingly, comparisons of the observations (whether from Raw or RR data) with their model equivalents are only made for those observations for which the influence of clouds is smaller than the 10 % threshold. (For other data the corresponding model observations were not available in the data sets used for this study).

1.2.1 Clouds with a small radiative impact and cloud free scenes

Particular caution is also needed when interpreting 1D-Var cloud parameters in situations where the cloud influence on the radiances is generally weak (very small cloud fractions or very low cloud). While many such situations are likely to correspond to cloud free conditions, the 1D-Var always assumes some finite values for CFr and CTP . These in some sense spurious cloud parameters may strongly depend on the noise. While for the use of the 1D-Var as a preprocessing system this ambiguity may actually not be really detrimental (the influence of such clouds is very weak anyway) one has to be careful interpreting statistics that contain such data.

2 Results

2.1 The data

The statistics presented below have been produced using 5 files from the Met Office data processing system. Each file contains IASI data from Metop A corresponding to a six hour time interval (all files together cover the 30 hour time interval: 01.11.2014, 0 UTC - 02.11.2014, 0 UTC). All radiances (original observations, RRs or model equivalents) included in this report had been converted to brightness temperatures. Apart from the raw radiances and corresponding RRs of the 314 channels processed by the Met Office system, the files contained processing information such as the Met Office's system quality flag and cloud parameters (cloud fraction, CFr and cloud top pressure, CTP) obtained from the 1D Var preprocessing system (and also those used to initialize the 1D Var assimilation).

From these data, first guess (FG) departures (i.e., observations minus the corresponding model first guess) and 1D Var analysis departures ("Obs-ANA", observations minus the corresponding value obtained from the 1D Var retrieval) could be computed, however, as explained above, only for data whose radiances (according to the 1D Var retrieval) are not affected by more than 10% through the presence of clouds. It has to be said that for radiances affected by clouds, the FG is actually not completely identical with the model background but the corresponding radiative transfer computations have been repeated (after the 1D Var step) using the retrieved values of CFr and CTP and the background profiles of temperature and humidity. The reason for this is to make sure that the bias correction, which is calculated from statistics compiled after 1D-Var, is consistent with the profile used as the background used in 4D-Var. As previously mentioned, in 4D-Var, the retrieved CFr and CTP are used for all RT calculations.

Regarding the short time reserved for this study, it was decided to restrict the analysis to bands 1 and 2 which means that 270 channels have been considered:

1. 165 channels (1-165) from band 1, 648.75 to 1142.5 cm^{-1}
2. 105 channels (166-270) from band 2, 1142.75 to 1927.25 cm^{-1}

The sensitivity functions of channels from band 1 tend to be higher peaking for smaller indices while the largest indices correspond to window channels. Channels from band 2 are sensitive to water vapor.

2.2 The presentation of data in bins of cloud variables

The statistics are mostly presented below in 3 pannels with 9 graphs [labeled (a)-(i), respectively] where each graph corresponds to a different subset (or bin) of the observational data. Data are either binned according to cloud fraction (CFr) or cloud top pressure (CTP) values as retrieved by the 1D Var system. These cloud variables can be either obtained using raw data (CFr_{Raw} , CTP_{Raw}) or reconstructed radiances (CFr_{RR} , CTP_{RR}). The corresponding CFr or CTP intervals are given in the respective graphs. As explained above, the 1D Var attributes a non zero (positive) cloud fraction to all scenes and, therefore, cloud free scenes generally correspond to very small (but non zero) cloud fractions. To cover such very small cloud fractions in the CFr bins, two bins with very small CFr values are used below. In the figures binned according to cloud fraction, graphs (b) and (c) correspond to the intervals $0 < CFr < 0.0001$ and $0.0001 < CFr < 0.08$, respectively.

Since small cloud fraction values tend to be spurious, some of the statistics presented below have been restricted to scenes with $CFr > 0.7$. Similarly, low level clouds tend to be not very well constrained by the observations as their impact on the IASI radiances is relatively weak. For the 1D Var systems, it is therefore difficult to properly distinguish between low level clouds and cold surface temperatures (i.e., strongly negative first guess departures in surface temperature) and/or large (positive) humidity first guess departures of low level humidity. To avoid spurious (i.e., badly constrained) clouds, some of the statistics presented below have been restricted to $CTP < 700hPa$.

Further, the main topic of this report is to search for evidence indicating that the signal of a low level cloud may be aliased into higher peaking reconstructed radiances for which the corresponding raw radiances have no sensitivity to the cloud. To look for such evidence more directly, statistics corresponding to situations with $600hPa < CTP < 800hPa$ have been collected and are presented in section 2.5.2.

2.3 Cloud parameters retrieved from RR and from Raw data

Cloud fractions retrieved from RR and from Raw data are strongly correlated with an overall correlation of 0.986 (see top left graph of Fig.1 which corresponds to all observed scenes). Generally the correlation is higher for high peaking clouds (above 0.99) which is consistent with the fact that those clouds constrain the radiance spectrum more strongly (and therefore leave less ambiguity to the retrieval scheme).

The slightly lower correlation (of 0.986) in the highest bin ($CTP_{Raw} \in [0hPa - 200hPa]$) stems mostly from a number of outliers with very small values of CFr_{Raw} (< 0.05) for which CFr_{RR} is substantially larger. As discussed above, for lower peaking channels, small cloud fractions at high altitudes (i.e., small CTP) have a qualitatively similar impact as larger cloud fractions further down. It is therefore likely that one has $CTP_{RR} > CTP_{Raw}$ for this group of outliers (since the CFr_{RR} is larger). Indeed, looking at graph (b) of Fig.2 (where data are partitioned into CTP_{RR} and not CTP_{Raw} bins) these outliers do not exist (which means that $CTP_{RR} > CTP_{Raw}$ holds indeed for these outliers in Fig.1(b)). Instead Fig.2b exhibits a similar group of outliers but for very small values of CFr_{RR} (which apparently have $CTP_{RR} < CTP_{Raw}$ since these points are not included in Fig.1b).

Generally for bins which correspond to relative high cloud tops, outliers tend to be more frequent in the upper left half of Fig.1 (and in the lower right half of Fig.2) while for the lowest cloud tops (graphs (h and i)) there are more outliers in the opposite halves of the respective graphs. This is consistent with the assumption that $CFr_{RR} > CFr_{Raw}$ ($CFr_{RR} < CFr_{Raw}$) is typically together with $CTP_{RR} > CTP_{Raw}$ ($CTP_{RR} < CTP_{Raw}$). This assumption also seems useful for explaining differences when comparing the outliers structures of the graphs of Fig. 3 with those of Fig. 4. Figures 3 and 4 show cloud top height (i.e., CTP) scatter plots presented in bins according to cloud fraction intervals (corresponding to CFr_{Raw} and CFr_{RR} in Figs.3 and 4, respectively).

These results emphasize the importance of the employed sampling conditions when interpreting statistics which are sensitive to outliers. Below, most of the statistical results will actually not be very sensitive to outliers. On the contrary, most of the presented results will be robust with respect to whether bin intervals are defined with respect to cloud parameters retrieved from RR or Raw data. In some cases, however, where the number of available observations for some channels are quite small, results will be strongly dependent on whether CTP_{Raw} or CTP_{RR} is used for defining the respective bins.

Figs. 3 and 4 also show that, compared to the cloud fractions, correlations of cloud top heights are smaller. One reason for this are the data with extremely small cloud fractions ($CFr_{Raw} < 0.08$) a large part of which probably correspond to cloud free scenes. For higher cloud fractions, CTP is generally much better correlated. An exception to this are virtually fully covered scenes ($CFr_{Raw} > 0.99$) for which low clouds are seen to dominate the statistics. (These low clouds constrain the radiance spectrum to a much lesser extent.)

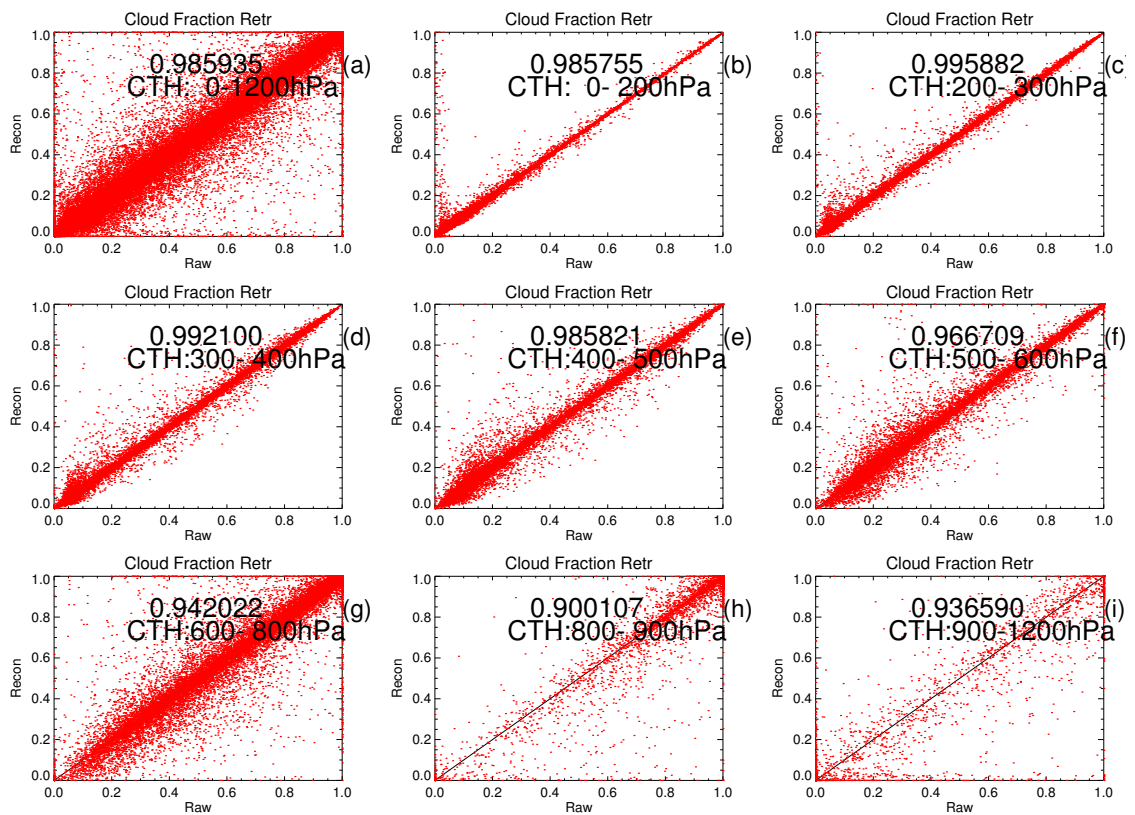


Figure 1: 1D Var cloud fractions retrieved from raw radiances (x-axis) and reconstructed radiances (y-axis). As indicated, different graphs correspond to different intervals of *CTP*. The *CTP* values used in this figure are taken from 1D Var retrievals using raw radiances. The numbers written in the graphs above the *CTP* intervals are the correlations of the respective data sets. Graph (a) contains all available data.

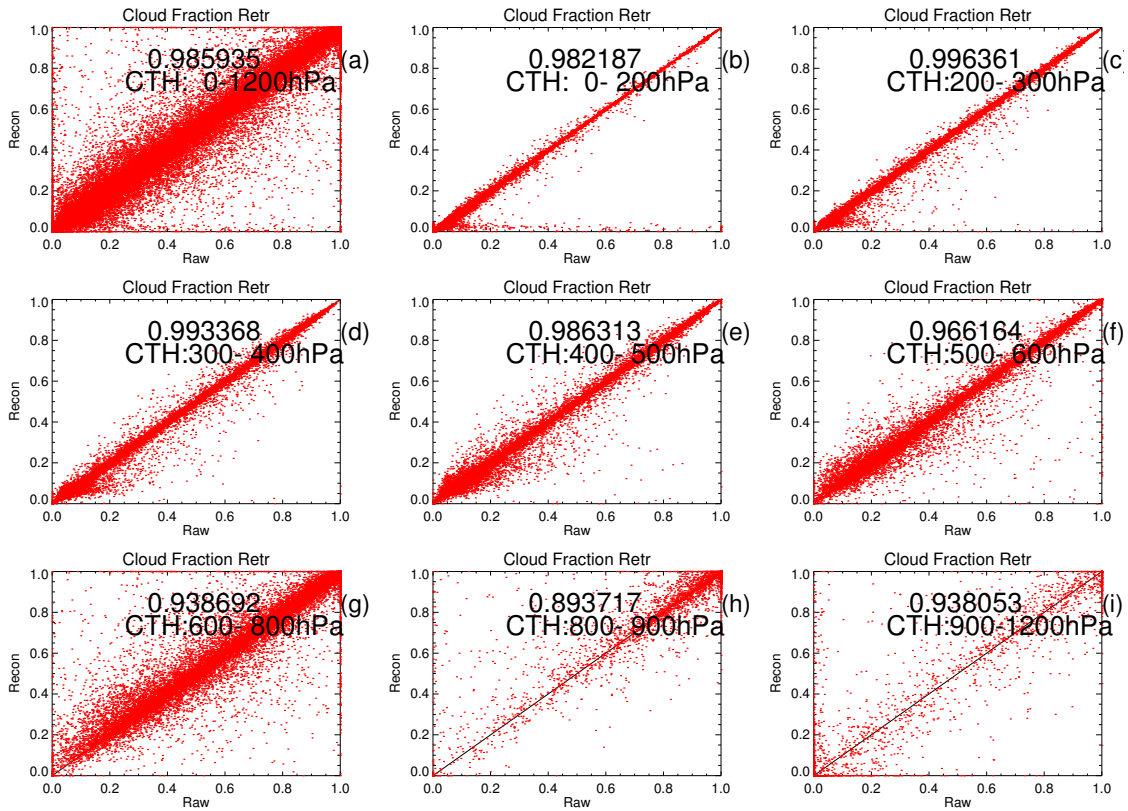


Figure 2: The same as Fig.(1) apart from the fact that cloud top heights (CTP_{RR}) retrieved from reconstructed radiances have been used to sample the data for the respective graphs.

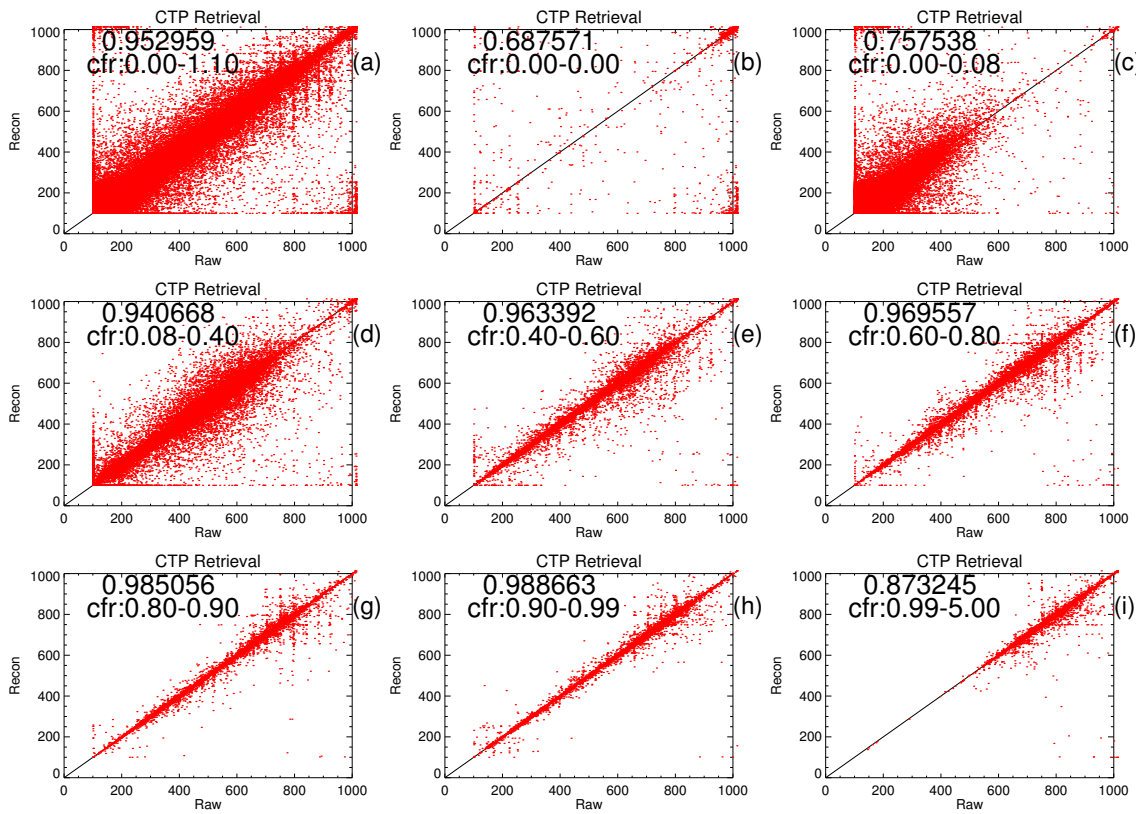


Figure 3: Similar scatter plots as in Fig.(1) but for clout top heights instead of cloud fraction. Different graphs correspond to different intervals of CFr (retrieved from raw radiances) as indicated in the respective graphs.

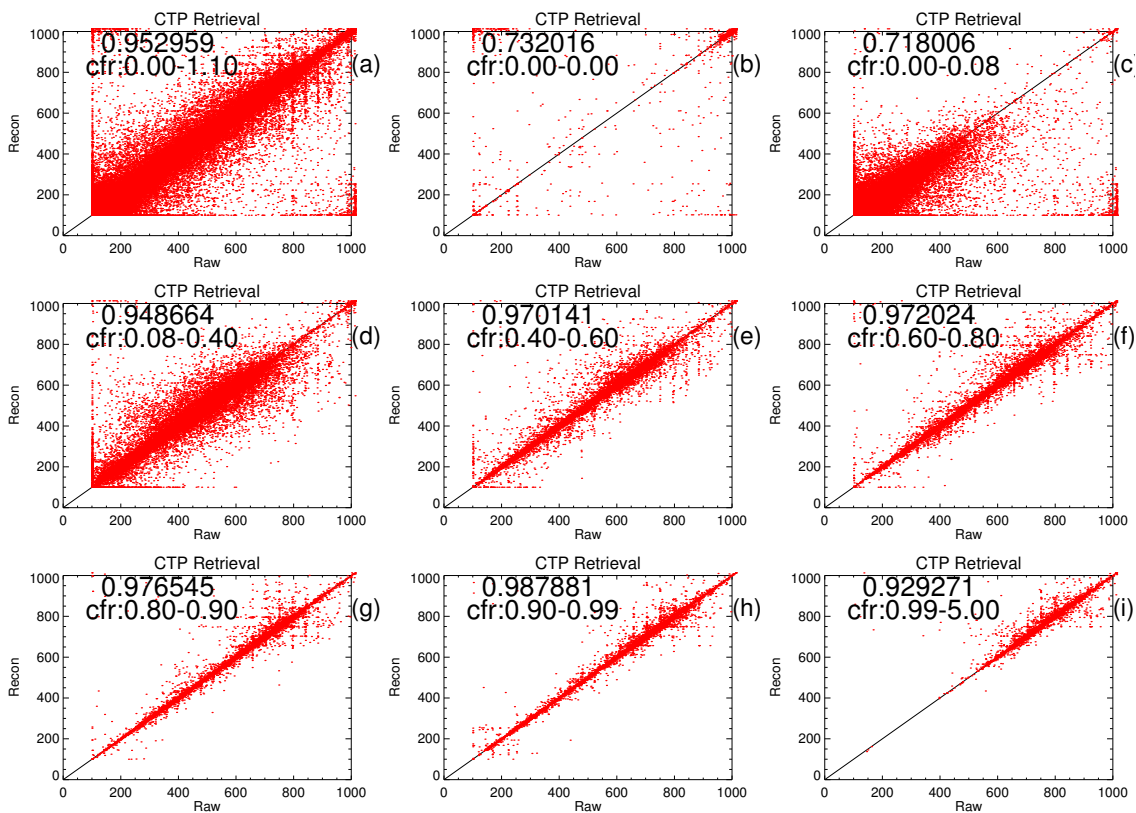


Figure 4: The same as Fig.(3) apart from the fact that CFr retrieved from reconstructed radiances have been used to sample the data for the respective graphs.

2.4 The residuals (RR - Raw)

Figure 5 shows the mean (top pannels) and the StDev (bottom pannels) of the residuals between RR and Raw radiances. Different graphs correspond to different cloud fraction intervals¹. Note that the top left graphs (graphs a) show the global statistics, i.e., they include all data.

For temperature channels (band 1), the graphs in Fig. 5 show the largest StDev of for the high peaking (stratospheric) channels with another little peak for the very low peaking and window channels (channel numbers around 145-165) from band 1. For band 2, the StDev is smallest for the smallest channels and then fluctuates quite strongly but on average increases with larger channel numbers.

While the qualitative behaviour of the different StDev curves in Fig. 5 is quite similar, there are systematic quantitative differences which are seen more clearly when subtracting the global statistics (as given by graph a) from each of the curves (see Fig.6).

One finds that the strength of the maximum for very low peaking and window channels from band 1 is quite sensitive to the cloud fraction bin. More precisely, the strength of the maximum generally increases with cloud fraction (apart from closed cloud decks, as seen in graph(i)). The effect is slightly stronger when excluding lower clouds ($CTP_{Raw} > 700$) from the statistics (see Fig.7 where only situations with $CTP_{Raw} > 700$ are included). Statistics on data binned according to cloud top height show a similar trend, provided small cloud fractions are excluded from the statistics (which apparently otherwise dominate the statistics). From Fig.8 (which is restricted to data with $CFr_{Raw} > 0.7$) the strength of the maximum is seen to increase with the altitude of the cloud top.

Generally, the residuals for the lower peaking channels of band 1 are larger the more the radiances (in the respective bins) are affected by clouds (i.e., the larger the cloud fractions and the higher the cloud tops are). Also the individual channels are seen to exhibit larger residuals the lower their sensitivity height is (for channels in band 1, the height of the sensitivity functions generally decreases with increasing channel index). This strongly supports the assumption that the residuals between RR and Raw radiances are larger in cloudy than in clear air².

Apparently the differences between raw and reconstructed radiances are larger in cloudy than in clear air (with the exception of fully covered scenes) and the question is whether this means that what is removed from the cloudy radiances by the PC analysis is only noise or whether also some part of the signal is removed. While this can not be judged from such statistical data alone, it is not implausible that radiance affected by clouds could be more noisy (the noise could result, e.g., from 3d effects at cloud edges or uneven cloud tops). This would mean that PC analysis *should* remove more from cloud affected radiances. Also, even if data from both regimes exhibited the same amount of noise, there is no guaranty that the PC truncation cuts off exactly the same amount of noise in different data regimes. This, however, does not mean that it cuts off part of the signal from the cloudy data regime. It could be that the RRs retain more noise in clear than in cloudy regions (i.e., more noise gets filtered out in cloudy regions).

¹These cloud fraction values are determined from the assimilation of the Raw data by the 1D Var. It should, however, be noted that the results presented in this subsection are largely independent on which data set was used in the 1D Var retrievals.

²While graph (i) for very low clouds formally seems to contradict this assumption, one finds from graphs (i) in Figs.3 and 4, that the bin of the highest cloud fraction is dominated by low level clouds whose impact on radiances is comparably low.

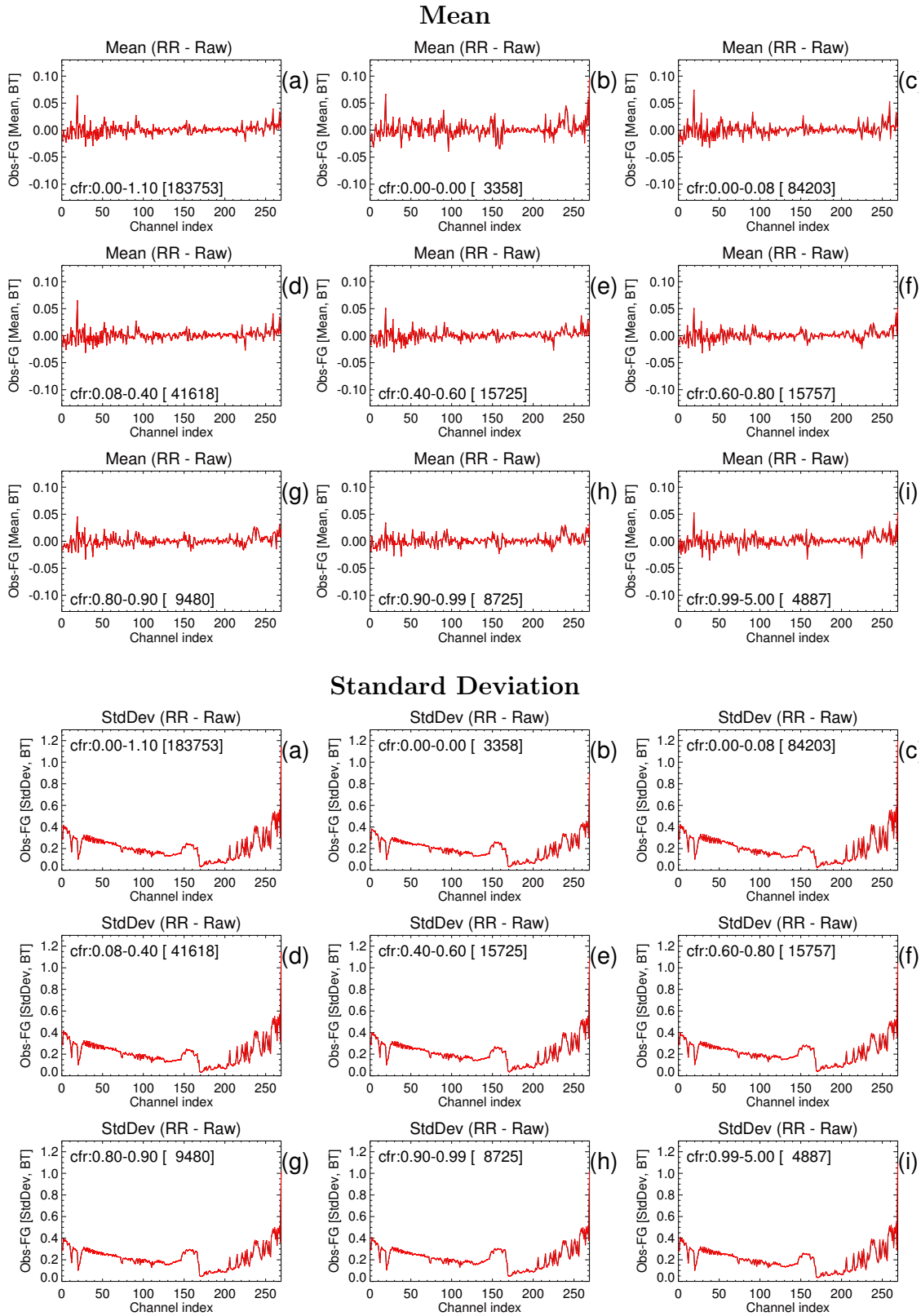


Figure 5: Mean (top) and standard deviation (bottom) of the residuals between reconstructed and raw radiances (in brightness temperature [K]). The cfr intervals given in the different graphs correspond to CFr_{raw} . The numbers in square brackets indicate the number of data in the respective bins.

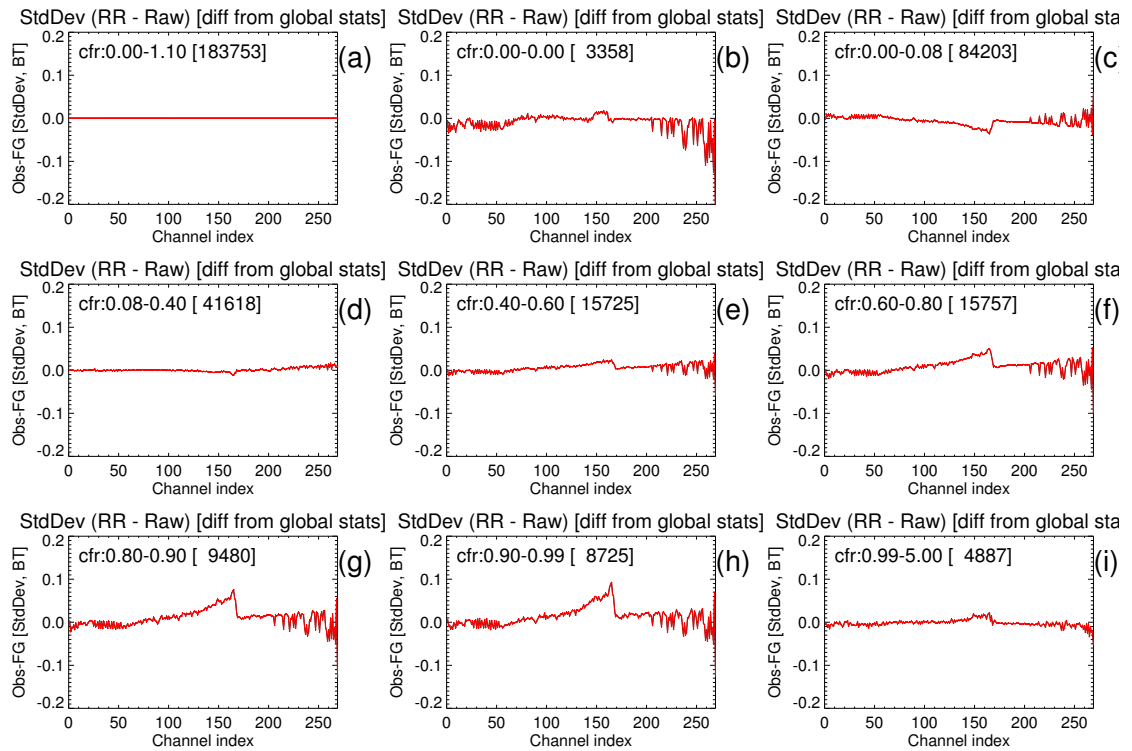


Figure 6: The graphs are equivalent with those from the 3 bottom panels of Fig.5 apart from the fact that the global statistics have been subtracted from the respective curves (the curve in graph a is consequently the zero line).

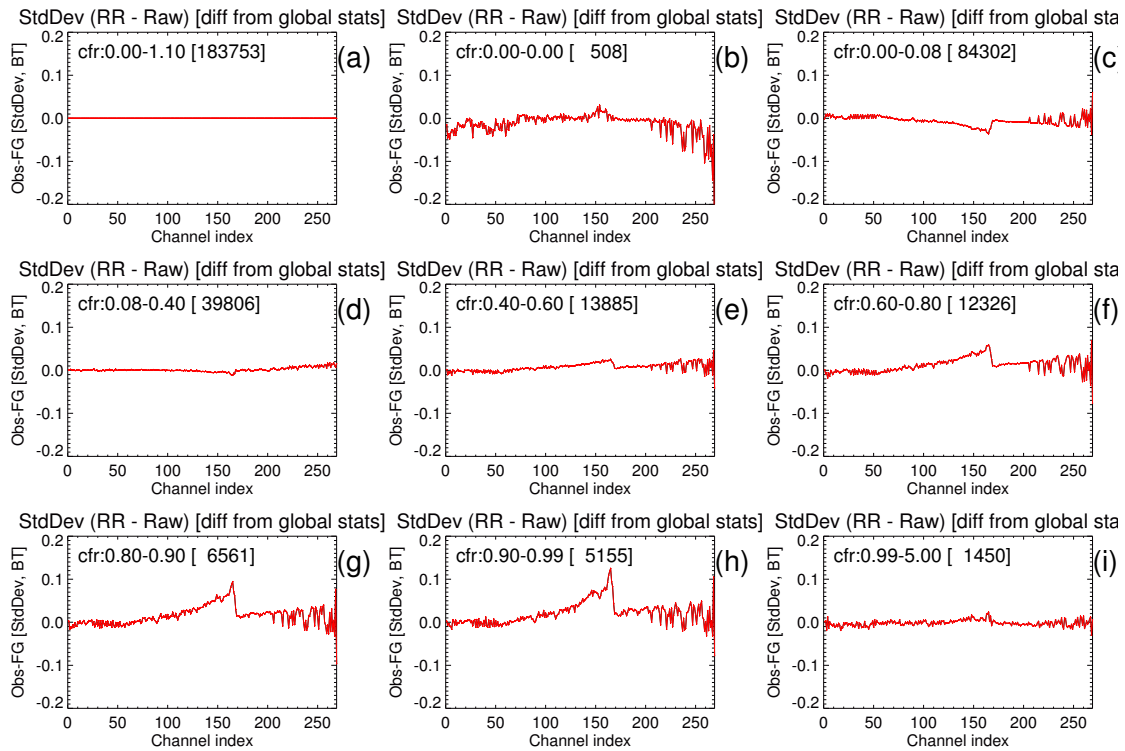


Figure 7: Similar to Fig.6 but only situations with $CTP_{raw} < 700hPa$ have been included in the computation of the StDev for the bins corresponding to graphs (b-i). Again the global StDev values (including all data, also with $CTP_{raw} \geq 700hPa$) have been subtracted from these curves.

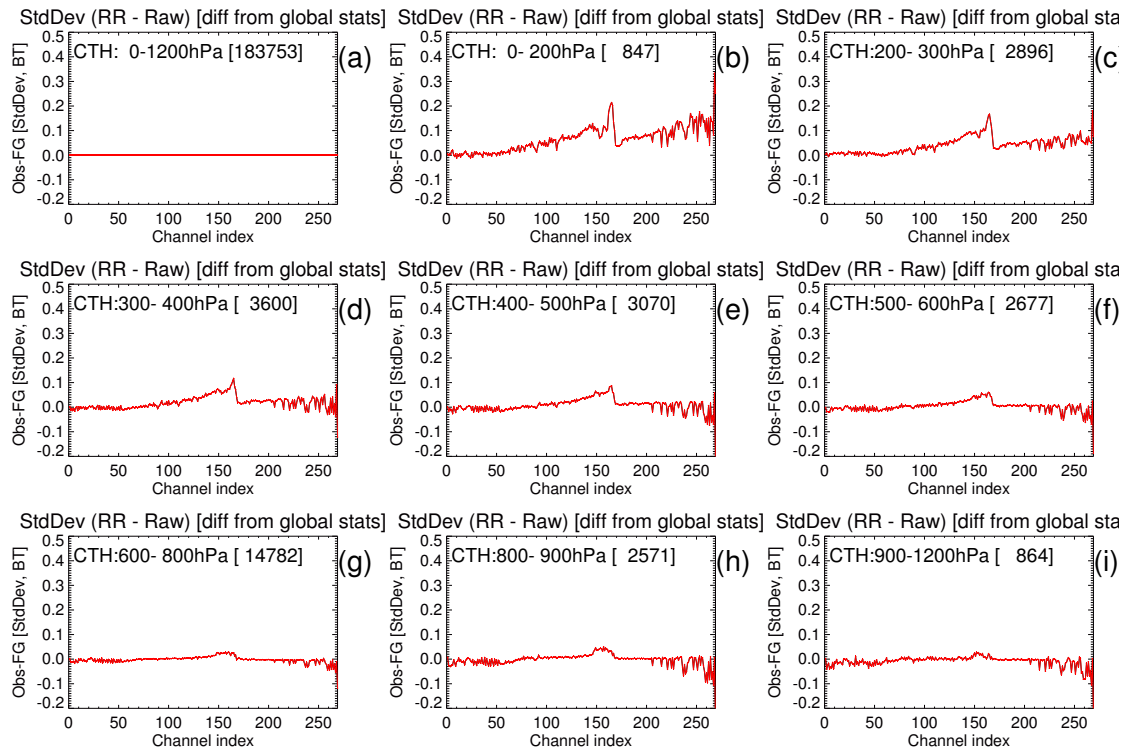


Figure 8: The same as Fig.7 but the bins are defined in terms of CTP_{raw} and the condition $CFr_{raw} > 0.7$ has been imposed for computing the StDev for the bins corresponding to graphs (b-i).

2.5 Comparisons with model observations

An important way of monitoring and testing observational data is the comparison with their model counterparts. The differences (increments) of the observations with the corresponding background values (Obs-FG) as well as the analysis values (Obs-ANA) are widely studied at operational centers and by the research community. In this study, statistics of Obs-FG and Obs-ANA increments have been computed for the different regimes of cloudiness discussed in the last sections. In the following, ANA corresponds to the 1D Var retrieval while the first guess (FG) is taken from the operational Met Office forecast (the Unified Model).

Since, as explained above, the data availability was not completely independent of the cloud properties (FG and ANA were not available for data affected more than 10 % by clouds) and since the retrieved cloud properties differ for retrievals based on reconstructed and raw radiances, respectively, the data coverage for Obs-FG departures is (slightly) different for the two data sets. When comparing statistics, it seemed, however, desirable to look at exactly the same observation subset for both data sets. Therefore, Obs-FG data were only included in the statistics presented below when they were available for the respective observation in *both* data sets. This ensures that when comparing Obs-FG (or Obs-ANA) statistics obtained from RR and Raw data, respectively, it can be excluded that observed differences are just a consequence of the different data availability in the two sets³.

2.5.1 Statistics depend on cloud top height

Regarding first raw radiances, Fig. 10 shows the corresponding mean and the standard deviation of Obs-FG and Obs-ANA increments binned according to CTP_{Raw} . The number of data used for the statistics⁴ can be seen in Fig. 9. The corresponding statistics involving reconstructed radiances show (at least qualitatively) good agreement (see Fig.11 which shows the corresponding statistics for RR data using exactly the same bins as in Fig. 10). In all cases, the retrievals (green curves) strongly reduce the Obs-FG bias and standard deviation. The standard deviation reduction for small channel indices (high peaking temperature channels from band 1) is clearly more efficient when using RR data which is consistent with the assumption that these data have a higher information content and less noise than the raw radiances.

To highlight some differences of the two data sets, Fig. 12 shows the differences between the Obs-FG statistics when computed from raw and reconstructed radiances, respectively (i.e., the red curves in Fig. 12 show the difference between the corresponding red curves in Fig.11 and those in Fig. 10). One finds that for high and medium high clouds the standard deviation of Obs-FG is smaller for RR than for Raw data which is consistent with the assumption that the residual between the data sets consists mainly of noise. For some lower clouds (graphs (g) and (h))⁵, however, for the low peaking channels (indices around 100-150) the StdDev is larger for RR than for Raw data while the bias is somewhat reduced for these data.

Since these are the channels whose sensitivity region is just above the assumed cloud, one might be tempted to take this as evidence that RRs of channels in the transition regions between cloud affected and clear channels could be systematically perturbed (the search for such evidence is the aim

³The data selection does, of course, depend on whether the cloud parameters defining the respective bins are retrieved from RR or Raw radiances.

⁴The data sets contain only radiances for which, in units of radiances, the influence of the retrieved cloud is less than 10%. Data are only taken if both RR and Raw data exist for the respective channels.

⁵Apart from the bin of the lowest clouds where the effect can not be observed.

of this investigation). One must, however, keep in mind that the data shown here contain a number of spurious clouds whose retrieved cloud parameters may depend strongly on noise and therefore are likely to differ considerably between Raw and RR data. The impression that (for these channels) RR data are more noisy than Raw data could therefore be a sampling problem. Indeed, looking at Fig. 14 which shows the same statistics but for data sampled according to CTP_{RR} (and not CTP_{Raw}), the regions where the StdDev difference of RR and Raw data is positive have disappeared in graphs (g) and (h). A small region where this happens is now visible for slightly higher clouds (graph (f): $500 < CTP_{RR} < 600$) for which this does not exist in Fig. 12. This supports the assumption that the observed larger variance of the RR data is linked to the particular sampling procedure.

Looking further at statistics where only scenes with $CFr_{Raw} > 0.7$ are considered (see Figs. 15, 16, 17 and 18), there are no channels for which the standard deviation of Obs-FG is larger for RR than Raw data apart in the lowest bin (see graph (i) of Fig.18 where $CTP_{Raw} > 900hPa$). As explained above, these low-level clouds (from the lowest bin) are also badly constrained by the IASI observations. Looking at the same statistics (i.e., restricted to $CFr_{Raw} > 0.7$) but sampled according to CTP_{RR} , this effect also disappears in the lowest bin (see Fig.19).

We conclude that the occurrence of channels (in certain CTP bins) for which the standard deviation of Obs-FG is larger for RR than Raw data is indeed strongly linked to the sampling procedure. In all cloud parameter bins where this is observed, spurious clouds (i.e., cloud parameters which are only weakly constrained by the observations) are likely to play an important role. For such clouds, the particular optimal values of CFr and CTP may strongly depend on the noise and therefore are likely to differ between RR and Raw data. In such cases, considering only observations for which, e.g., CFr_{Raw} is in a certain interval (but not necessarily CFr_{RR}) could easily introduce a bias by selecting more cases for which the 1D Var finds a CFr_{Raw} which gives a good fit of OBS-FG to the Raw data while a corresponding best value of CFr_{RR} is less optimal (the corresponding fit to the RR data is less good). Extreme caution is therefore required when drawing further conclusions from these statistics.

2.5.2 A closer look at scenes with low level clouds

The main topic of this work was whether scenes with low level clouds exhibit any suspicious features which could indicate that information from the low level cloud is in some way aliased into radiances which are not (or only very weakly) affected by clouds. To investigate this more directly, Figs. 20, 21, 22 and 23 show statistics restricted to situations which, according to the 1D Var retrieval, have a cloud with $600hPa < CTP_{Raw} < 800hPa$. One finds that the statistics obtained from raw radiance retrievals (Fig.21) are generally very similar to those were RR data are processed in the 1D Var (Fig.22). The only exception is the bin with extremely small cloud fractions ($CFr_{Raw} < 0.0001$, graphs (b)) where, as seen from Fig.23, the StDev of Obs-FG is larger for RR than for Raw data. Again, the increased StDev for RR data is caused by the sampling method and vanishes when the selection of bins is made according to RR data (see Fig.24). There is no evidence for an increase in residual for the RRs (i.e. in the RR residual as compared with the Raw residual) with increasing cloud fraction.

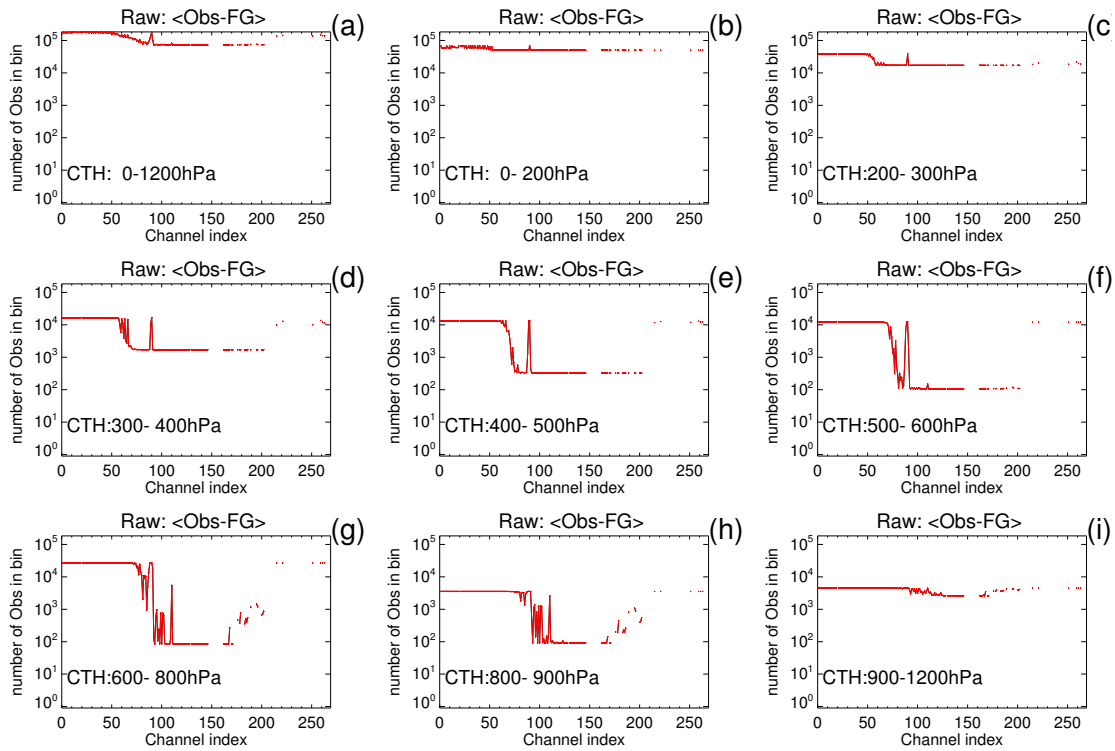


Figure 9: Number of data for the individual channels which (for the respective CTP_{Raw} bin) are included in the OBS-FG and Obs-ANA statistics presented in Figs. 10, 11 and 12.

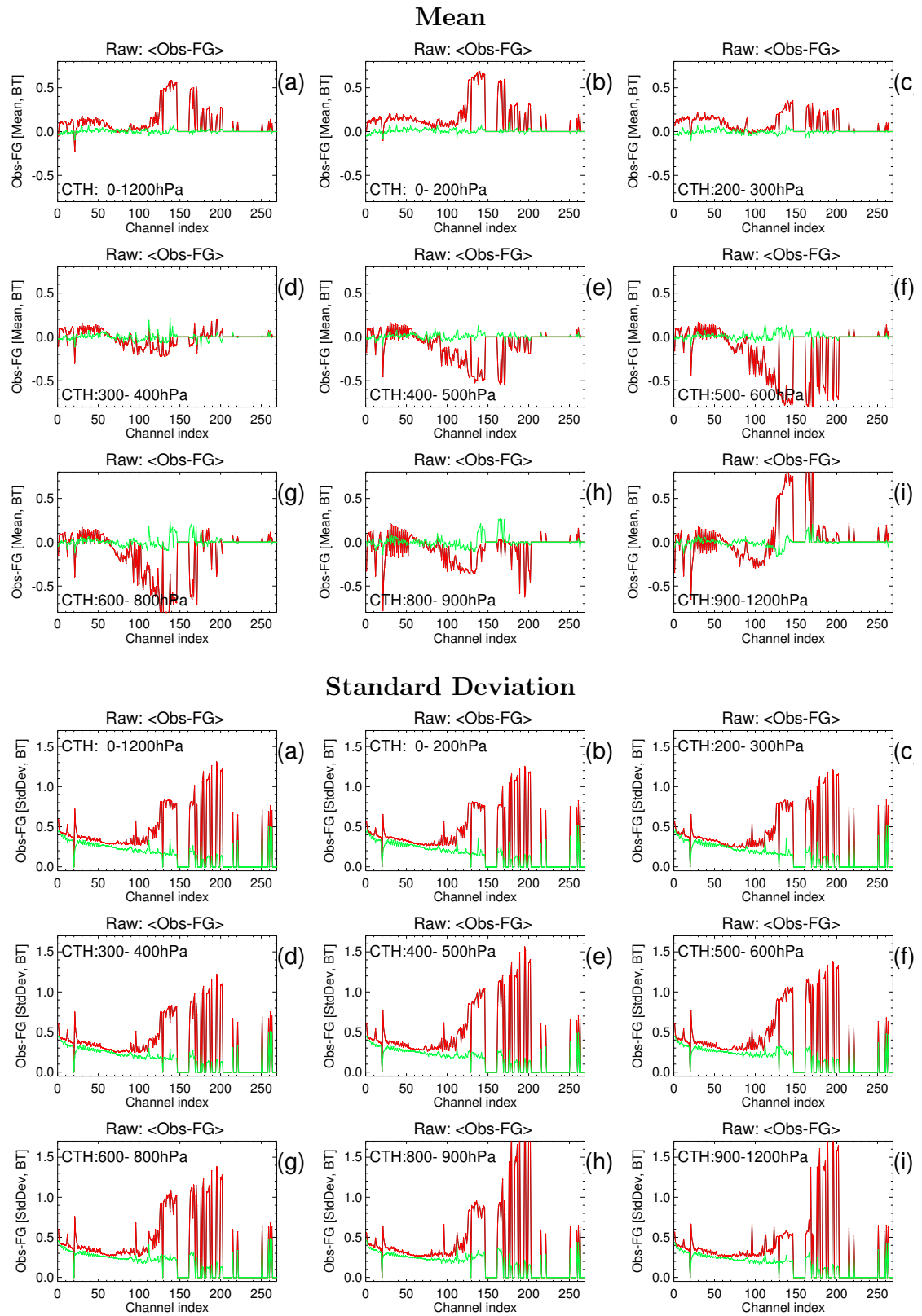


Figure 10: Mean (top) and standard deviation (bottom) of Obs-FG (red) and Obs-ANA (green) for raw radiances. Different graphs correspond to different CTP_{Raw} bins (as indicated by the CTH intervals).

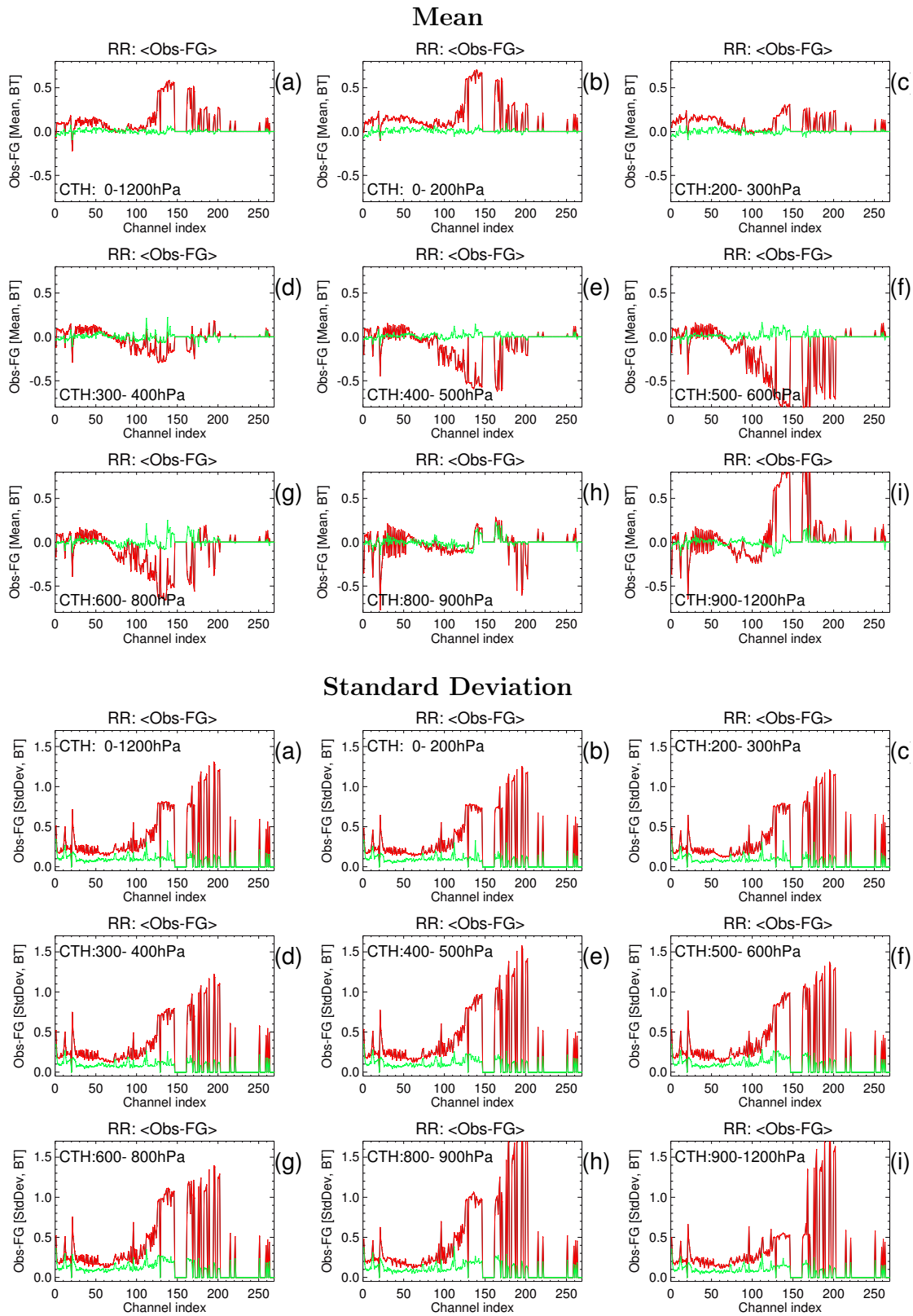


Figure 11: The same as Fig. 10 but for reconstructed radiances (but in the same CTP_{Raw} bins as used in Fig. 10).

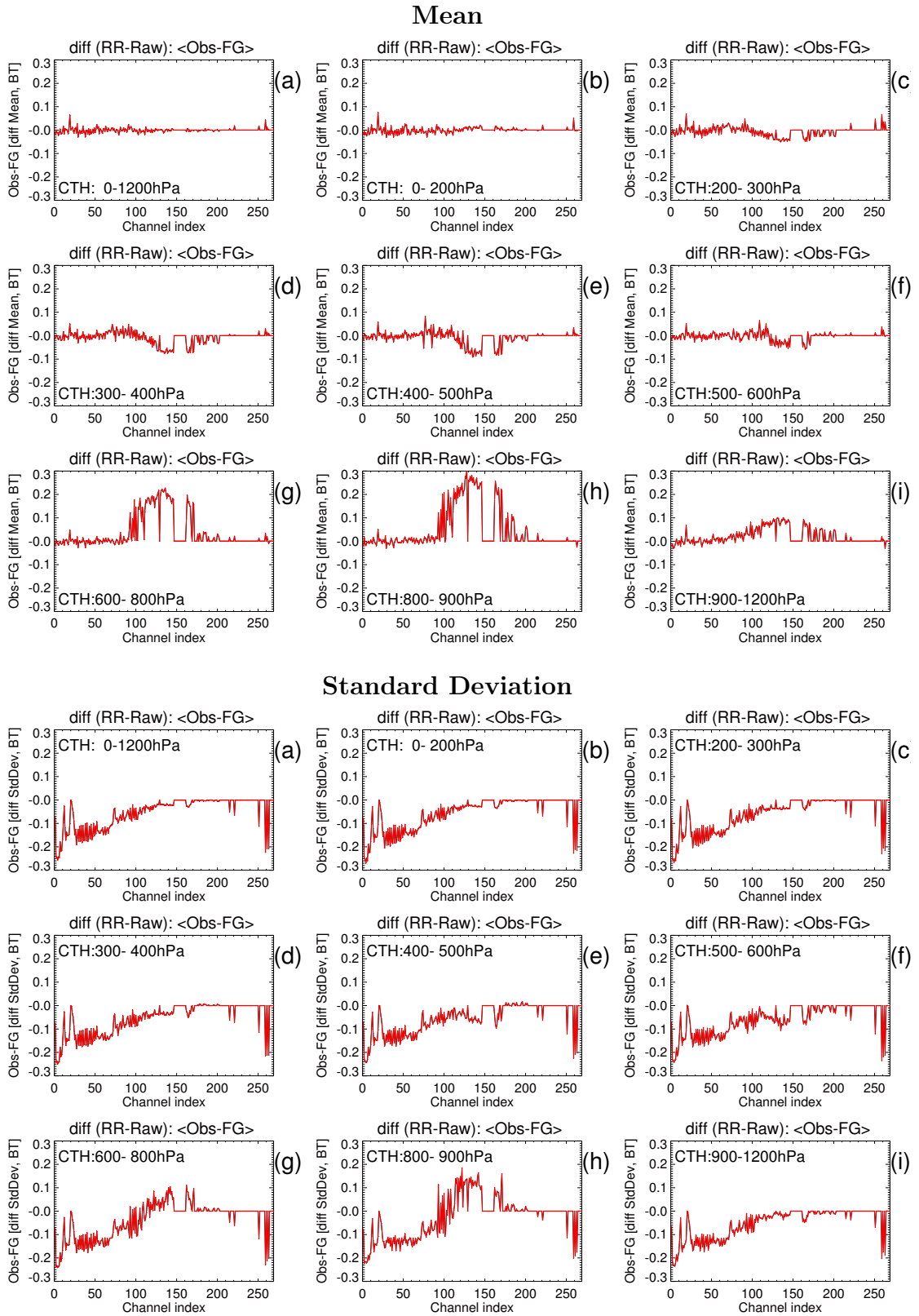


Figure 12: Difference of Obs-FG statistics derived from RR and Raw data, respectively. Top graphs show the difference between the means, bottom graphs between the standard deviations. Different graphs correspond to different CTP_{Raw} bins (the same bins as used in Figs. 10 and 11).

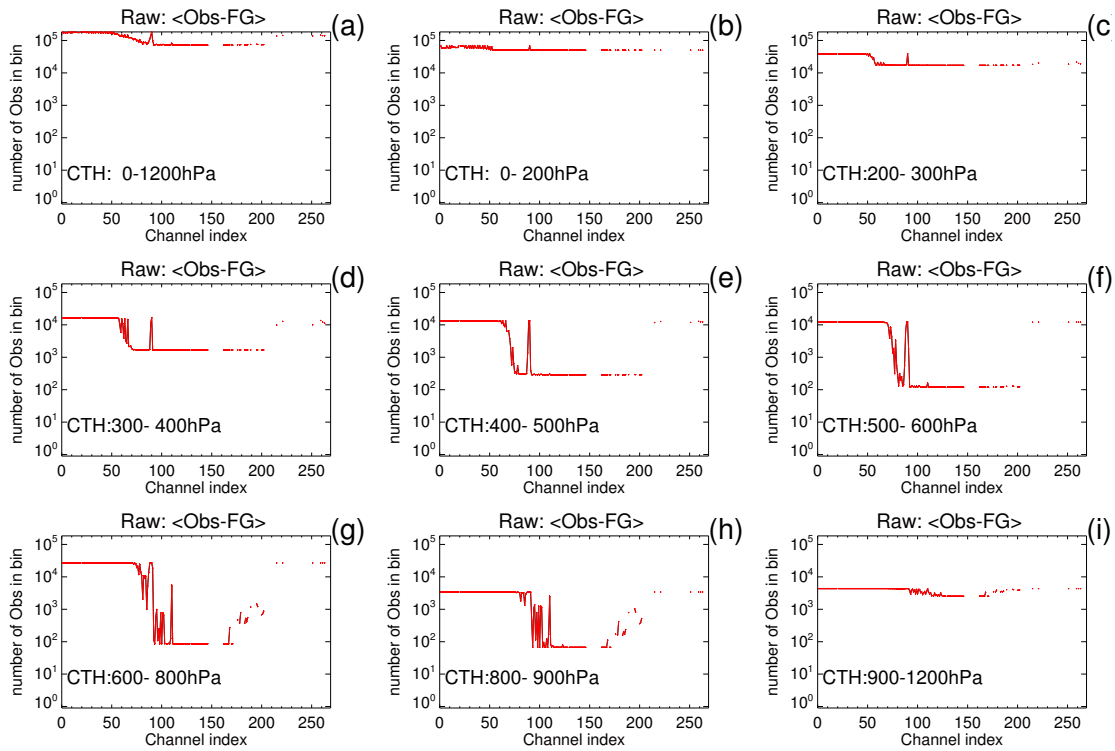


Figure 13: Number of data for the individual channels which (for the respective CTP_{RR} bin) are included in the OBS-FG and Obs-ANA statistics presented in Fig. 14.

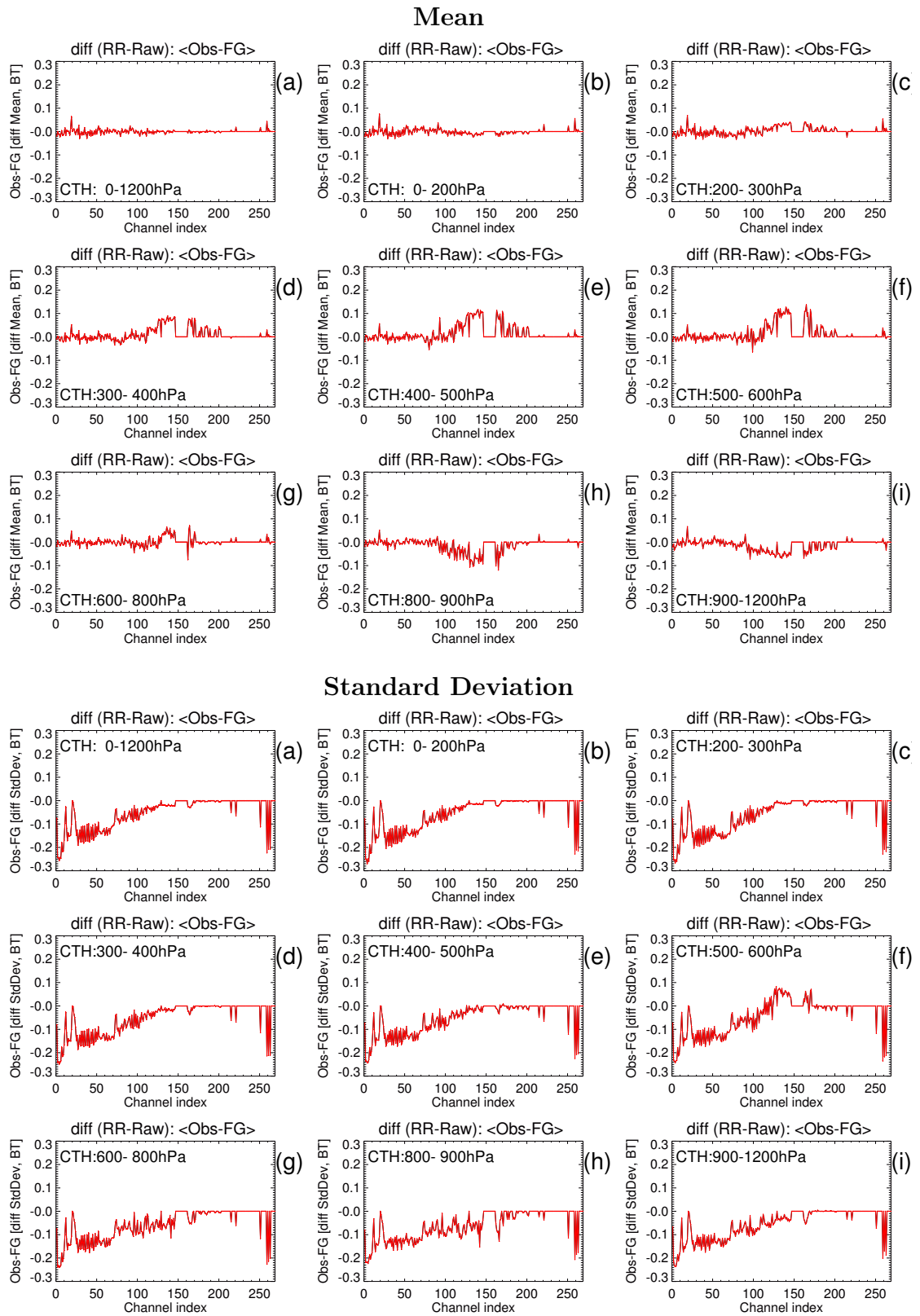


Figure 14: The same as Fig. 12 apart from the fact that the indicated CTH intervals correspond CTP_{RR} (and not CTP_{Raw} as in Fig. 12).

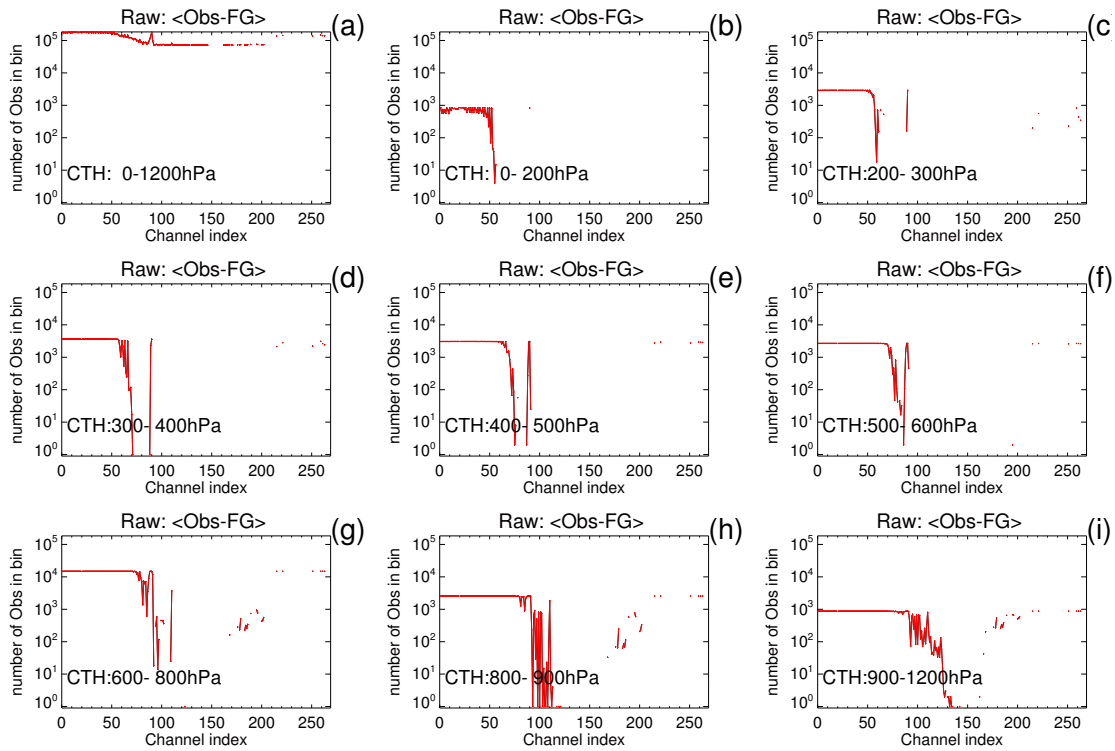


Figure 15: Number of data for the individual channels which (for the respective CTP_{Raw} bin) are included in the OBS-FG and Obs-ANA statistics presented in Figs. 16, 17 and 18.

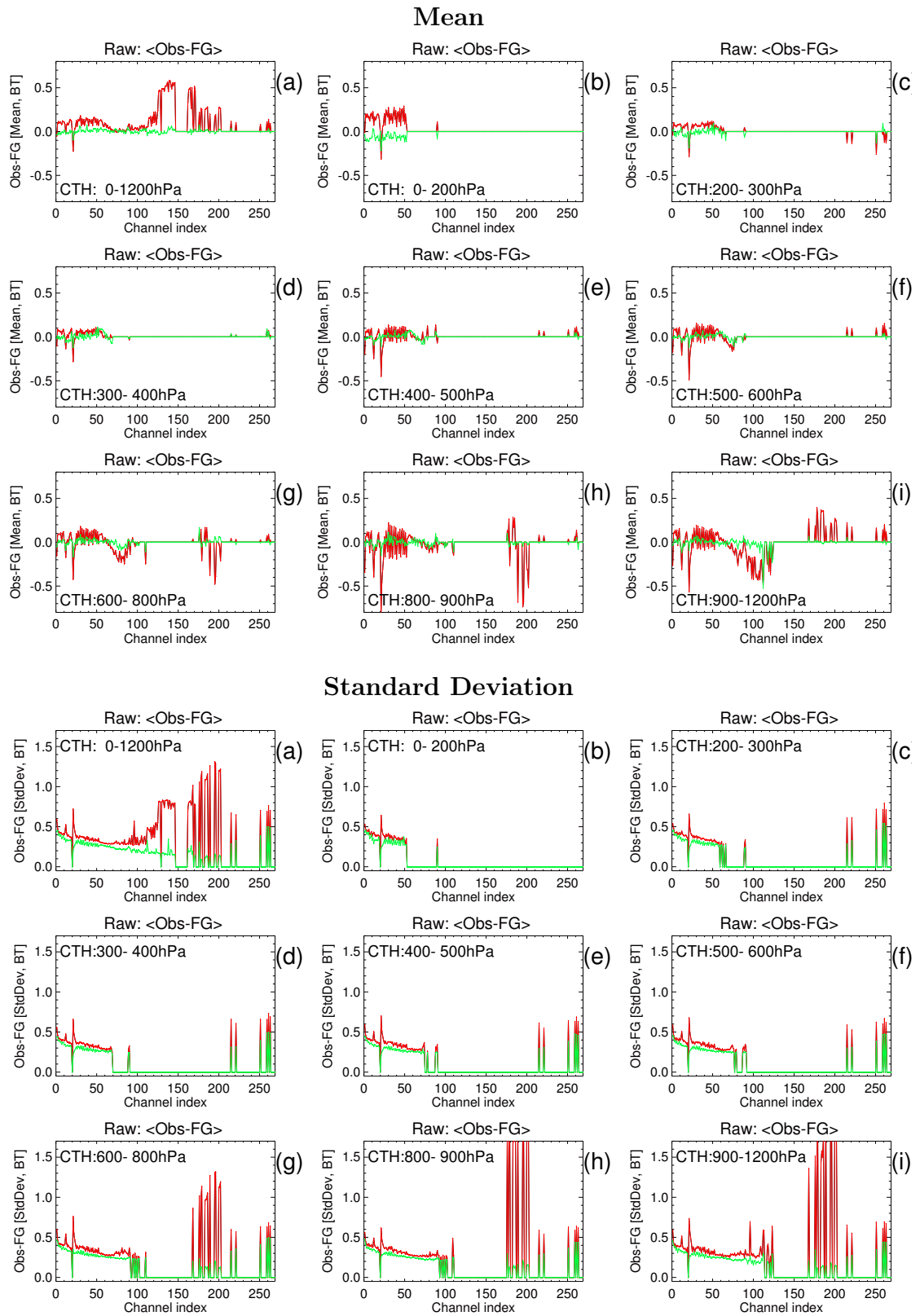


Figure 16: As Fig. 10 but restricted to data with $CFr_{Raw} > 0.7$.

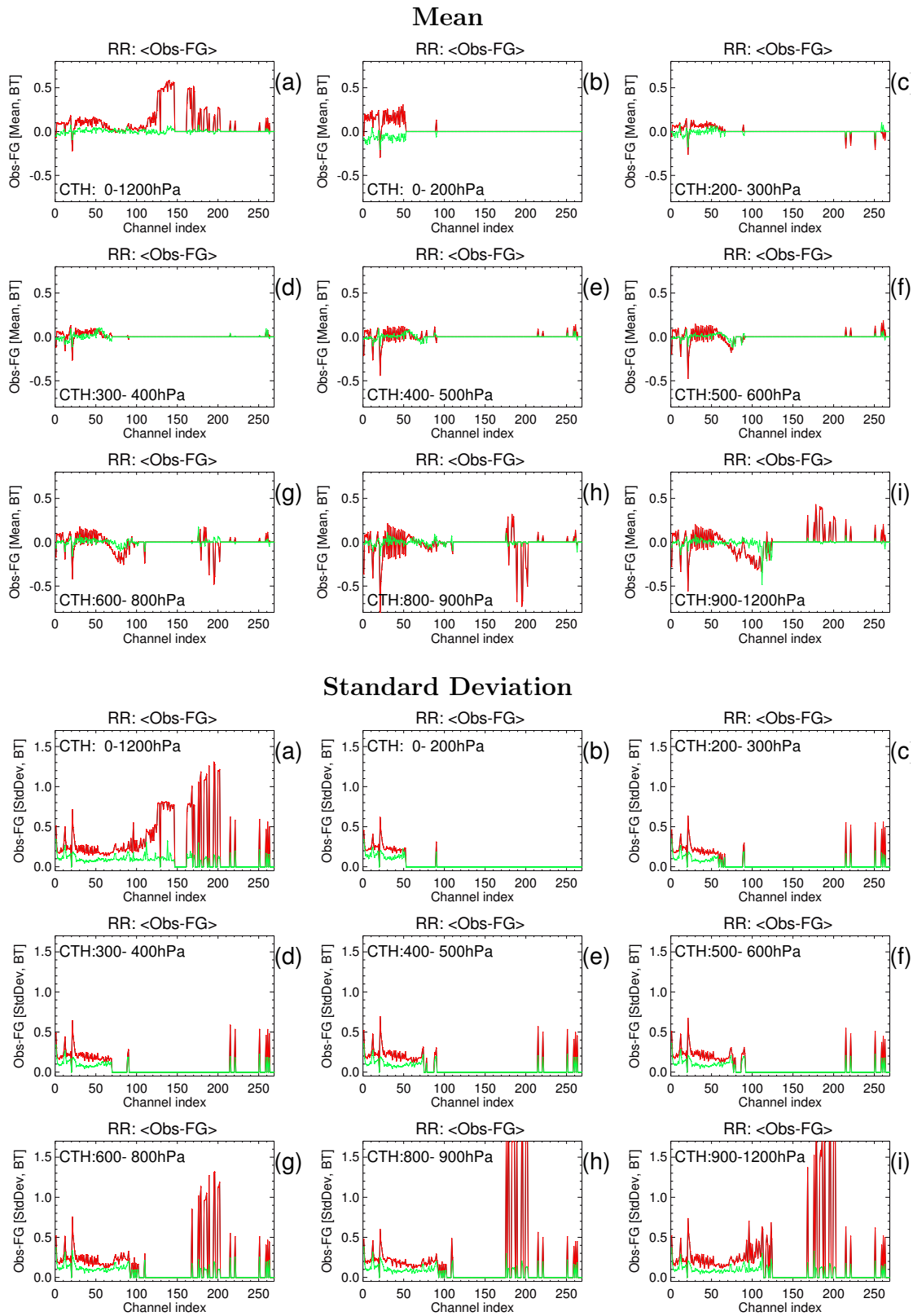
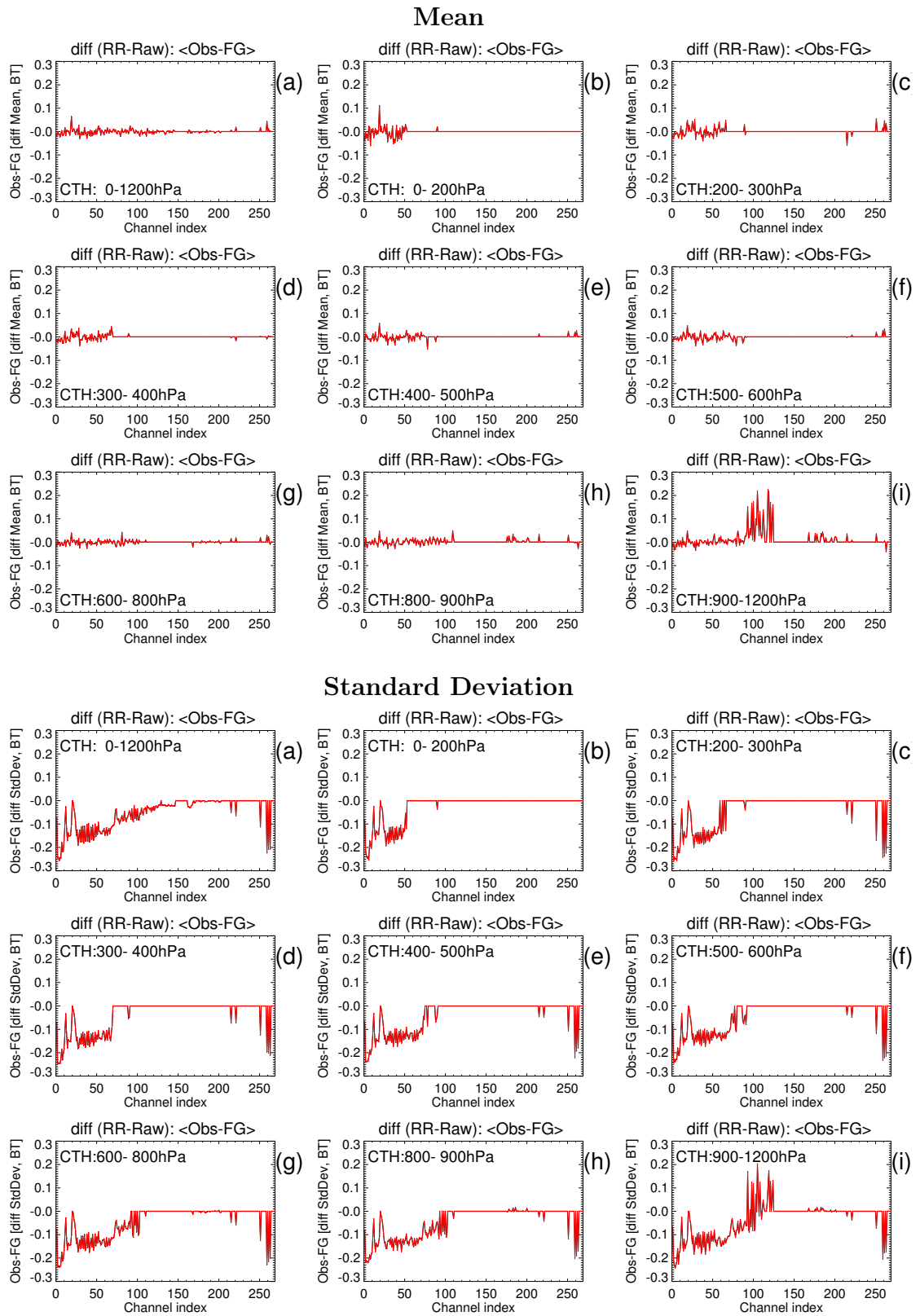
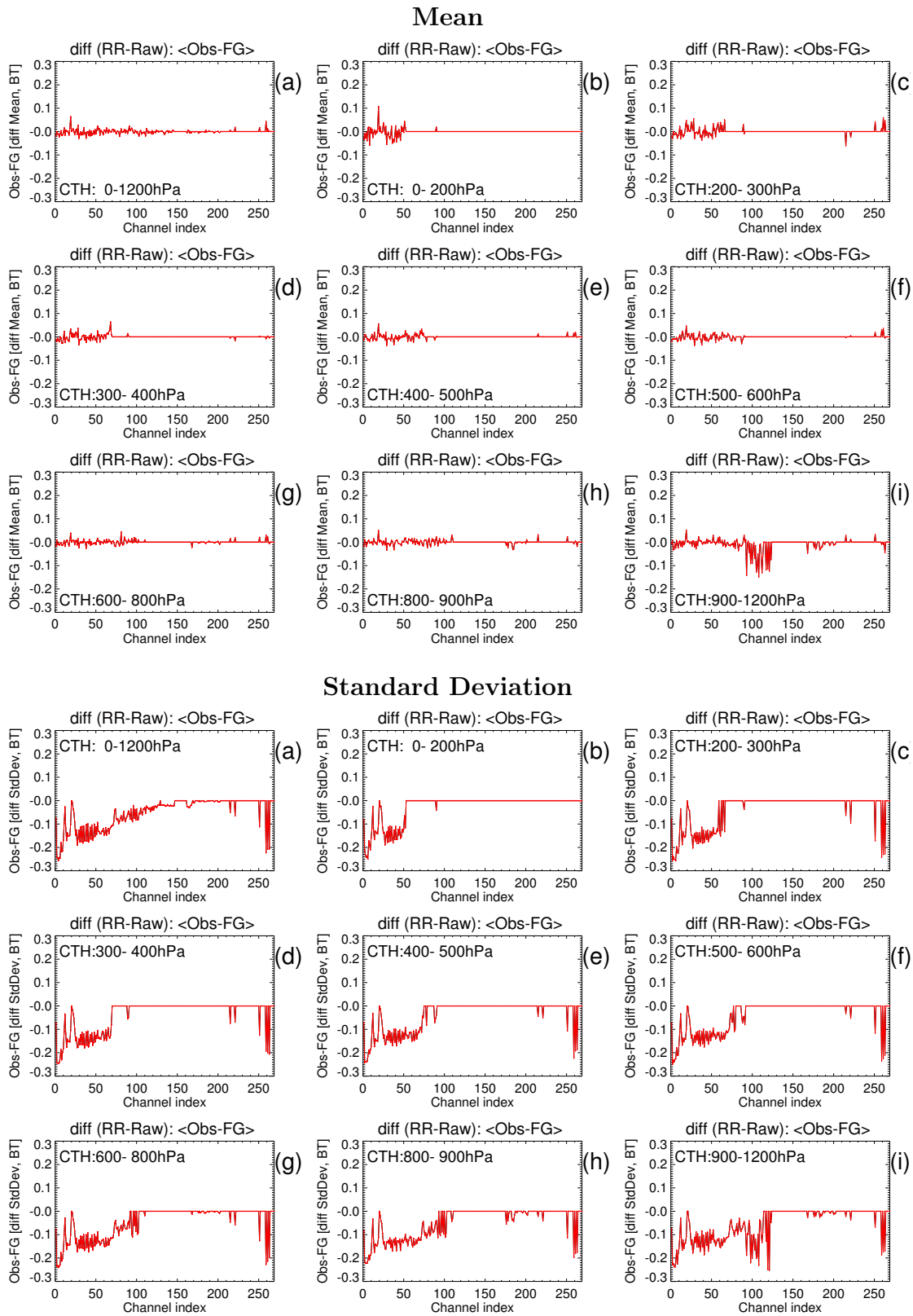


Figure 17: As Fig. 11 but restricted to data with $CFr_{Raw} > 0.7$.

Figure 18: As Fig. 12 but restricted to data with $CFr_{Raw} > 0.7$.



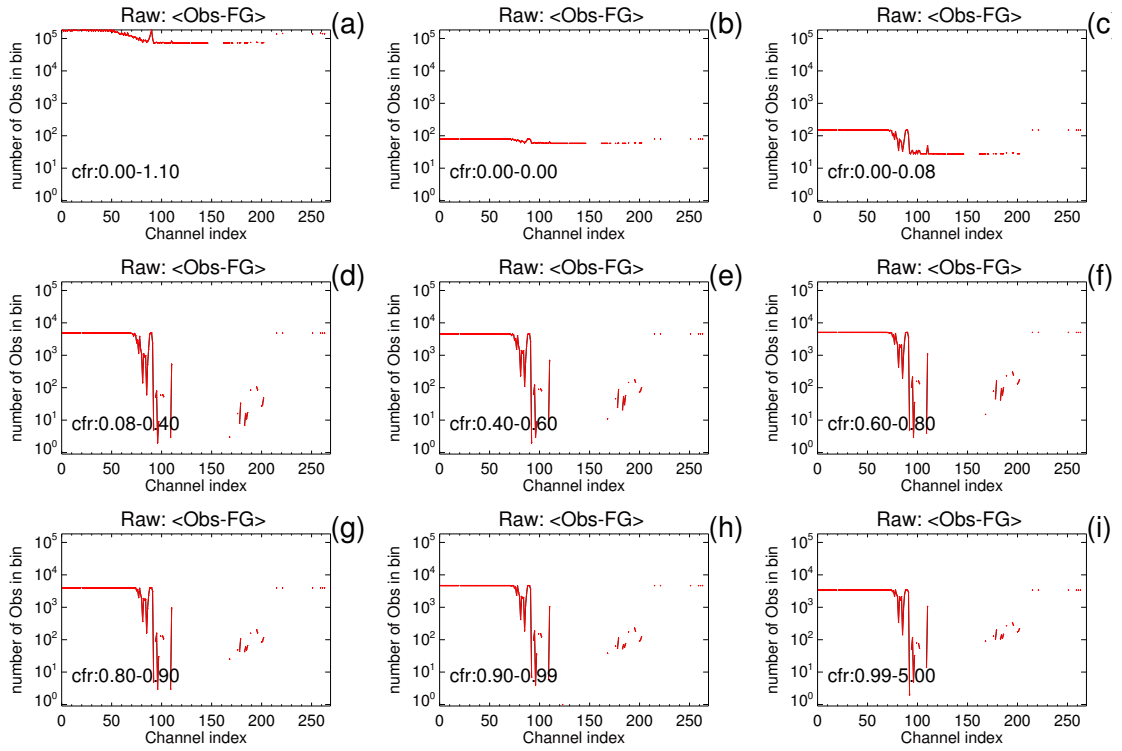


Figure 20: Number of data for the individual channels which (for the respective CFr_{Raw} bin) are included in the OBS-FG and Obs-ANA statistics presented in Figs. 21, 22 and 23 below.

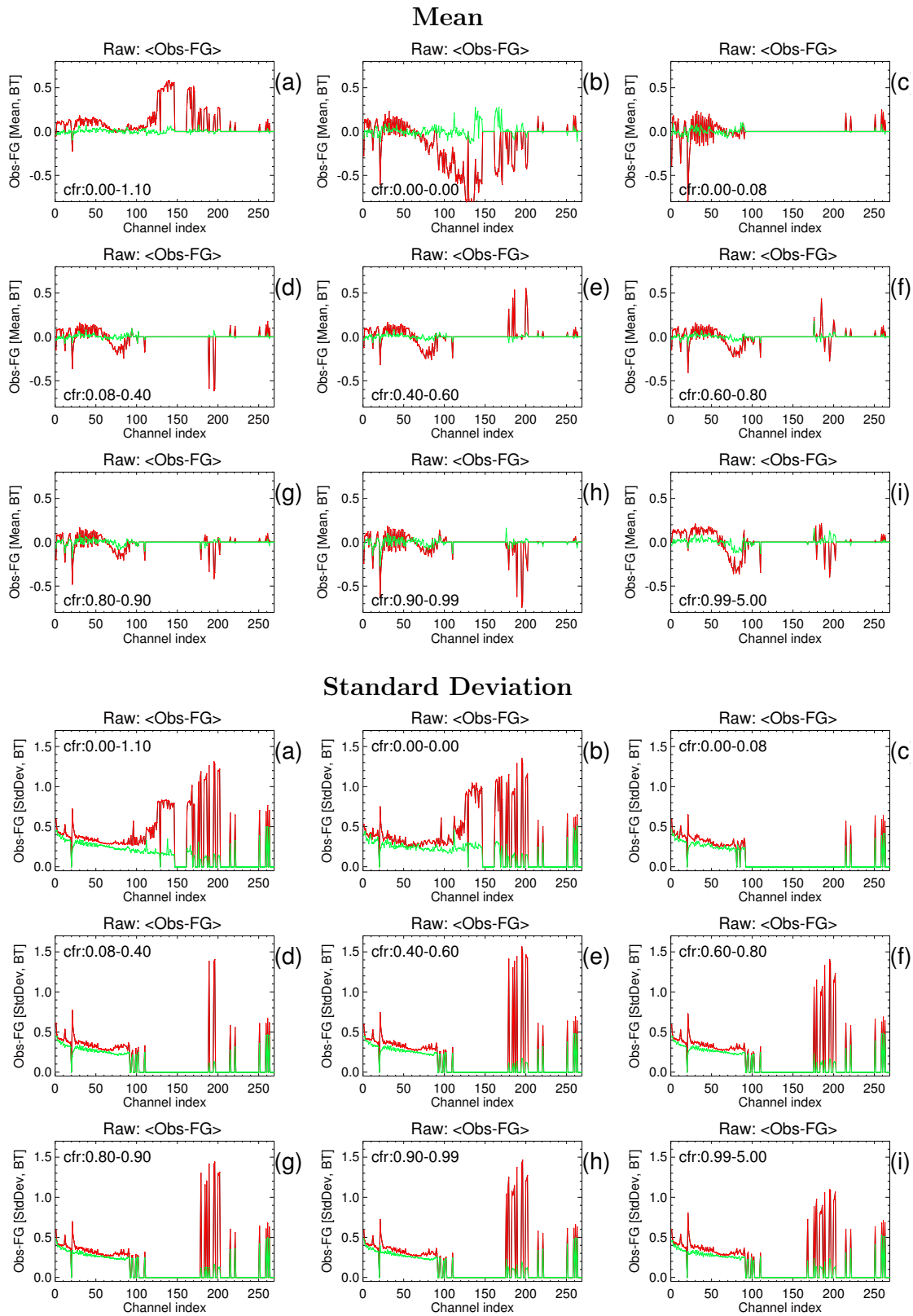


Figure 21: Similar to Fig. 10 but for CFr_{Raw} bins and restricted to data with $600hPa < CTP_{Raw} < 800hPa$.

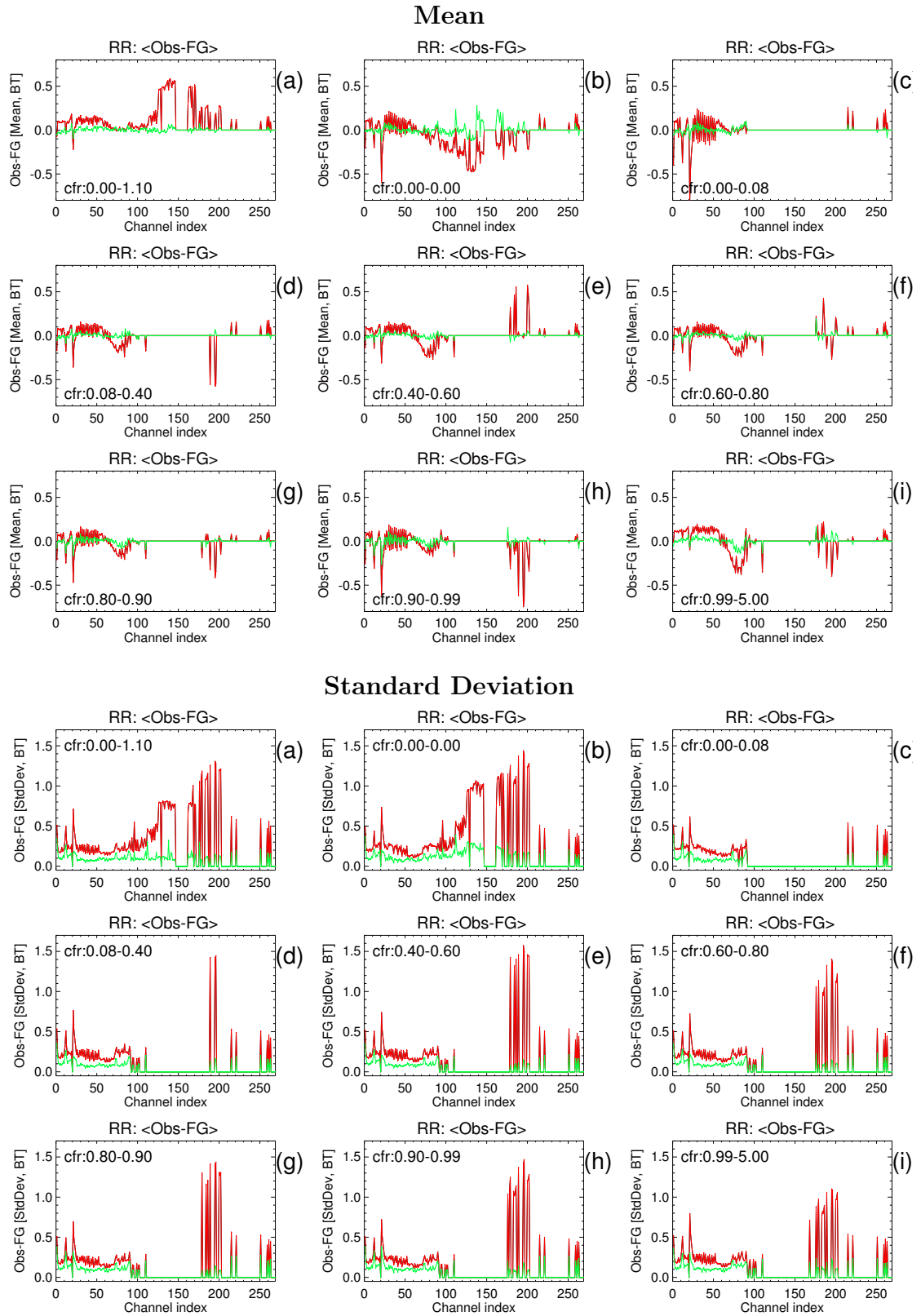


Figure 22: Similar to Fig. 11 but for CFr_{Raw} bins and restricted to data with $600hPa < CTP_{Raw} < 800hPa$.

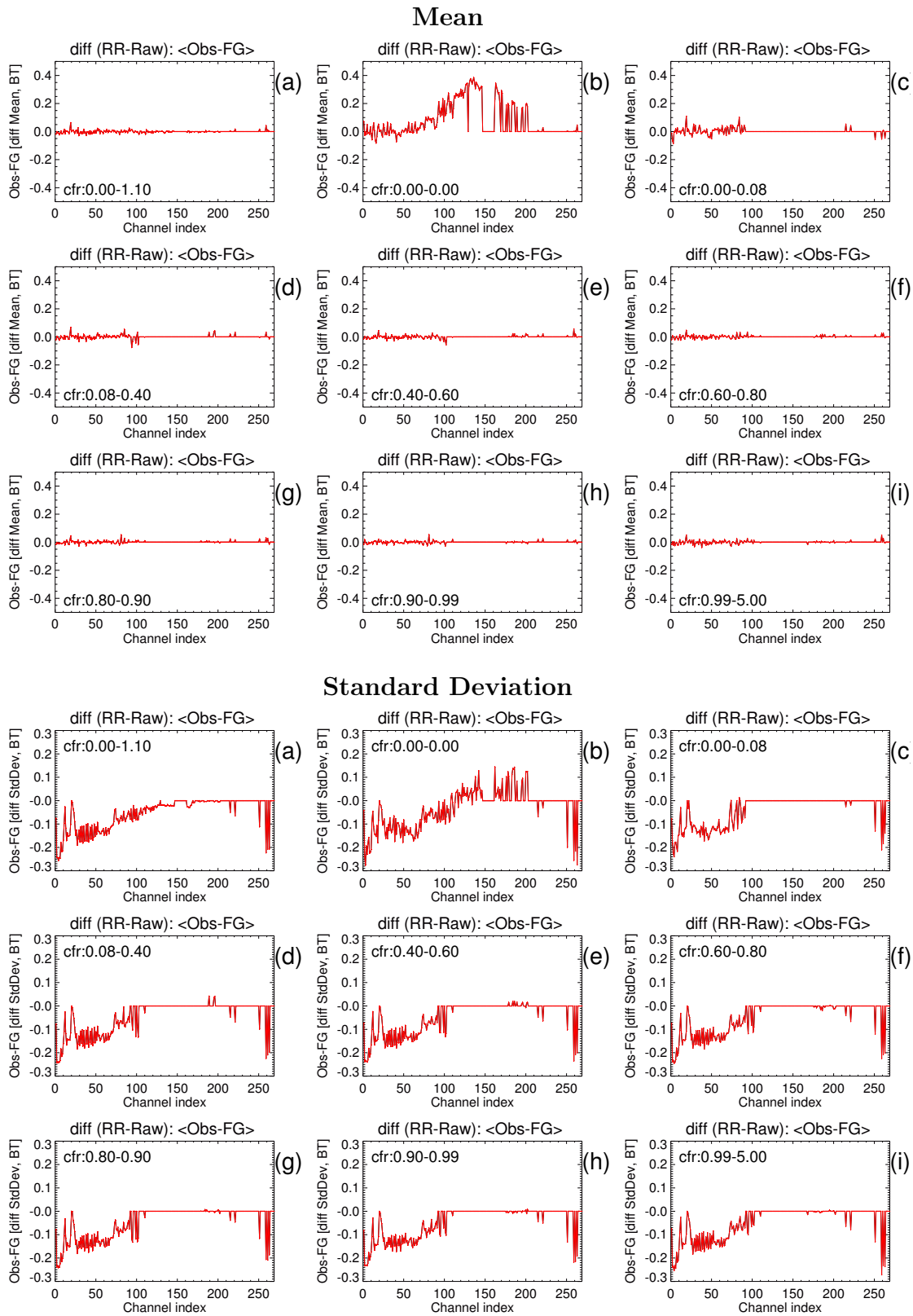


Figure 23: Similar to Fig. 12 but for CFr_{Raw} bins and restricted to data with $600hPa < CTP_{Raw} < 800hPa$.

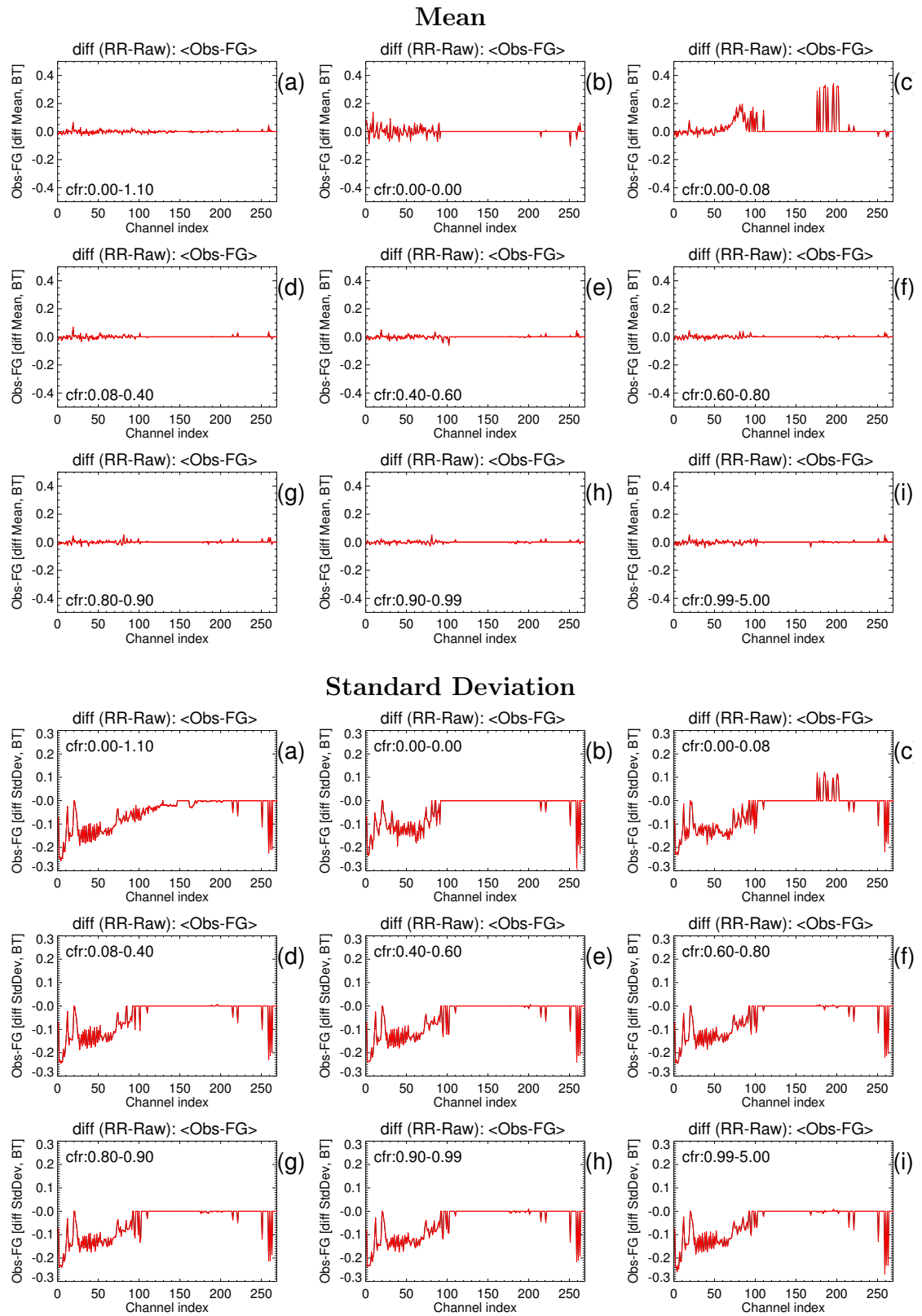


Figure 24: The same as Fig. 23 apart from the fact that the indicated cfr intervals correspond CFr_{RR} (and not CFr_{Raw} as in Fig. 23).

3 Summary and Conclusions

RR and Raw radiance have been compared for different cloudy conditions (as described by CFr and CTP). One aim of the study was to see whether there is evidence that, under certain cloudy conditions, RRs are less suitable for properly characterizing the Raw data. More precisely, the question originating this work was whether for channels for which the corresponding Raw observations are not affected by clouds the RRs may still be influenced by clouds which are below the levels to which a particular channel is sensitive. In principle, since RRs are computed as linear combinations of different channels, one should expect an RR to contain part of the cloud signal if any of the (raw) channels which contribute to the particular RR is affected by clouds (even if the raw radiance of the RR's nominal channel number has no sensitivity to the cloud). Of course, the effect may be extremely weak since only a limited number of raw channels contribute to a particular RR channel and also, since the transition between those channels which are significantly cloud affected and those on which the cloud has no influence at all, is not abrupt but continuous⁶.

To investigate this question, statistical properties of RR and Raw data were computed for different regimes of CFr and CTP . While some systematic variations of the data with cloud properties have been identified, strong evidence suggesting systematic differences between the data sets (which can not be explained by the fact that RRs contain less noise) could not be observed. Particularly, it was found that the residual between RR and Raw data is largest the more a particular data (sub-) set is affected by clouds (which seems at least qualitatively consistent with findings of Guedj et al. (2015)). That the residuals of a PC decomposition are different in different regimes is, however, not surprising but has to be expected. Further, it is not implausible that radiances affected by clouds could be more noisy than clear radiances, because of the effects of scene inhomogeneity on field effects within the interferometer, and the larger residuals of cloud affected radiances could mean that more noise is suppressed by the PC decomposition. Whether the larger residuals are really related to more noise can not be judged on purely statistical grounds (unless one has some further information as, e.g., independent observations).

Also, some suspicious features were observed for the Obs-FG statistics that could be linked to sampling problems. More specifically, in some data bins, Obs-FG increments were found to have a larger StDev for RR than for Raw data which could be linked to situations where clouds that are not well constrained by the observational data contribute significantly to the statistics. In this case the values of CFr and CTP derived from RR and Raw data, respectively, can differ strongly from each other (depending on the noise) and selection criteria based on parameters from one data set (say on CTP_{Raw}) may be strongly dependent on the noise. More robust statistics could, in principle, be obtained by restricting to situations where cloud parameters obtained from the different data sets agree sufficiently well. For this study this option had been discarded as this may exclude exactly those situations where RR data might have problems (i.e., situations we have tried to identify).

In conclusion, no really suspicious features could be found regarding the different types of statistics studied in this project. This further increases our confidence in the RR data. Of course, a statistical study can never prove that there might not be *some situations* where the quality of RR

⁶As discussed above, PC analysis is most suitable for describing collective features of a data set (i.e., those involving a larger number of channels). Therefore, if the transition is "sufficiently continuous" it should be well described within the PC approximation. However, the assumption here is that the "cloud affected-not cloud affected" transition is a little more abrupt than those resulting from most other signals (as, e.g., a temperature or humidity perturbation). Also, in contrast to, e.g., earth-surface influences or effects related to trace gases, the respective set of channels where this transition occurs varies strongly with the cloud top height so that the pattern has a smaller weight in a statistical analysis which is based on averages in observation space.

data could be diminished by the presence of clouds (i.e., situations which can not be detected with the employed methods). To investigate the question further, one could think of a more targeted statistical search that explicitly selects situations where the linear combination for a clear RR channel comprises cloud affected channels. To gather such statistics, more detailed information on the degree to which individual channels are affected by clouds would be required. Also, the interpretation of such substantially more sophisticated conditional statistics would probably require a lot of care. Future studies should possibly also include comparisons with other (independent) observational data when searching for systematic deficiencies in the RR data.

4 Acknowledgments

The 2 weeks stay of OS as a visiting scientist at the Met Office headquarter in Exeter is financed by the EUMETSAT NWP SAF program. OS would further like to thank the Met Office satellite group for the extremely warm welcome and friendliness during his short stay in Exeter.

References

- N. Atkinson, F. Hilton, S. M. Illingworth, J. Eyre, and T. Hultberg. Potential for the use of reconstructed iasi radiances in the detection of atmospheric trace gases. *Atmospheric Measurement Techniques*, **3**(4):991–1003 (2010).
- S. Guedj, V. Guidard, and J.-F. Mahfouf. Preliminary studies towards the use of iasi pc products in the météo-france global data assimilation system (2015).
- F. Hilton, R. Armante, T. August, C. Barnet, A. Bouchard, C. Camy-Peyret, V. Capelle, L. Clarisse, C. Clerbaux, P.-F. Coheur, et al. Hyperspectral earth observation from iasi: Five years of accomplishments. *bulletin of the american meteorological Society*, **93**(3):347–370 (2012).
- F. Hilton, A. Collard, V. Guidard, R. Randriamampianina, and M. Schwaerz. Assimilation of iasi radiances at european nwp centres. In *Proceedings of Workshop on the assimilation of IASI data in NWP, ECMWF, Reading, UK*, pp. 6–8 (2009).
- M. Matricardi, F. Chevallier, G. Kelly, and J.-N. Thepaut. An improved general fast radiative transfer model for the assimilation of radiance observations. *Quarterly Journal of the Royal Meteorological Society*, **130**(596):153–174 (2004).
- E. Pavelin, S. English, and J. Eyre. The assimilation of cloud-affected infrared satellite radiances for numerical weather prediction. *Quarterly Journal of the Royal Meteorological Society*, **134**(632):737–749 (2008).
- R. Saunders, M. Matricardi, P. Brunel, S. English, P. Bauer, U. O’Keeffe, P. Francis, and P. Rayer. Rttov-8 science and validation report. *NWP SAF Report*, **41** (2005).